

SEPARATION OF METALS AS HYDRIDES
FROM LIQUID METAL SOLUTIONS

by

Paul Fred Woerner

A Dissertation Submitted to the
Graduate Faculty in Partial Fulfillment of
The Requirements for the Degree of
DOCTOR OF PHILOSOPHY

Major Subject: Metallurgy

Approved:

Signature was redacted for privacy.

In Charge of Major Work

Signature was redacted for privacy.

Head of Major Department

Signature was redacted for privacy.

Dean of Graduate College

Iowa State University
Of Science and Technology
Ames, Iowa

1960

TABLE OF CONTENTS

	Page
I. INTRODUCTION	1
II. APPARATUS	20
A. Vacuum System and Reactions Chamber	20
B. Sampling Devices	26
C. Furnace and Temperature Control	29
III. EXPERIMENTAL	30
A. Materials	30
B. Experimental Procedure	32
C. Chemical Analysis	36
1. Determination of thorium in magnesium	36
2. Determination of yttrium or lanthanum in magnesium	37
3. Determination of yttrium in zinc and of yttrium in magnesium-zinc alloys	39
4. Determination of cerium in magnesium	40
5. Determination of calcium and zirconium	40
IV. EXPERIMENTAL RESULTS	42
A. Hydride Reactions for Group IIA Elements	43
B. Hydride Reactions for Group IIIA Elements	48
C. Hydride Reactions for Group IVA Elements	65
D. Hydride Reactions for the Rare Earth Metals	68
E. Hydride Reactions for the Actinide Metals	72
V. THERMODYNAMIC CALCULATIONS	80
VI. DISCUSSION OF RESULTS	88
VII. SUMMARY	92
VIII. DETERMINATION OF THERMODYNAMIC PROPERTIES OF INTERMETALLIC COMPOUNDS FROM HYDRIDE REACTIONS	95
A. Introduction	95
B. Apparatus and Experimental Procedure	98
IX. EXPERIMENTAL RESULTS	107
X. THERMODYNAMIC CALCULATIONS AND DISCUSSION	113

XI. SUMMARY	119
XII. LITERATURE CITED	121
XIII. ACKNOWLEDGMENTS	126

I. INTRODUCTION

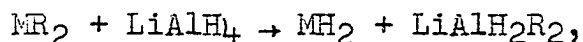
In recent years considerable research has been done to devise new methods for purifying or separating impurities from liquid metals, and particularly to develop new pyrometallurgical methods for reprocessing irradiated nuclear fuels (1, 2). Gas-metal reactions as a method of refining liquid metals has been employed by the metal industry for some years. In these processes the most reactive impurities are preferentially oxidized by the gas to form stable volatile or insoluble compounds which can be removed from the molten metal. Gas-metal reactions of this nature employing the halogen gases, oxygen and air have been extensively used in the purification of lead and iron (3). Very little research has been done on reactions involving hydrogen as a means for separating impurities from liquid-metal solutions. It is the purpose of this investigation to examine the potential for such reactions.

Hydrogen will enter into chemical combination with almost all the known chemical elements to form a variety of compounds known as hydrides. Paneth (4) originally classified the hydrides into the volatile hydrides, salt-like hydrides and the metal like hydrides on the basis of their comparative properties. Gibb and Hurd prefer to classify the hydrides as ionic, covalent, transitional metal and borderline hydrides (5, 6). Their classification is based on the crystal

structures, physical properties, chemical bonding and chemical behavior of the hydrides. This latter classification will be adopted in the following discussion. The ionic hydrides are salt-like compounds in which the hydrogen is present as the negatively charged hydride ion, H^- . This ion comprises a hydrogen nucleus, or proton, associated with a pair of electrons, and it is formally analogous to a halide ion. Only those elements which are strongly electro-positive are sufficiently strong reducing agents to transfer electrons to the hydrogen atom and thereby form the ionic or saline hydride. It is generally agreed that the alkali metals and the alkaline earth metals form hydrides of this type. Dialer (7) suggests that the metal-hydrogen bonds in the rare earth hydrides (MH_2) are also ionic. Libowitz and Gibb (8) have asserted that this ionic bonding can be extended to also include the hydrides of Group IIIA, IVA metals, the rare earth metals and the actinide series. Because of the strong electrostatic forces holding the aggregate of positive and negative ions together, considerable amounts of energy are required to separate the ions of these compounds. Thus the ionic compounds are generally solids which exhibit high melting points, high heats of formation, and a high degree of thermal stability.

The covalent or gaseous hydrides, include the hydrides of metals found in Groups IIIB, IVB, VB, VIB, and VIIB. Hydrides belonging to this group are of the electron-sharing

type and are characterized by low melting points, low heats of formation and a low degree of thermal stability. The covalent hydrides are generally gases or liquids at room temperature and are prepared by metathetical reactions. Although beryllium and magnesium are electropositive elements, they do not tend to form ionic hydrides. These two elements are generally classified with the covalent hydrides. They do form solid hydrides of definite stoichiometric composition, and may be considered as a bridge between the ionic and the covalent hydrides, since they exhibit intermediate properties between these groups. MgH_2 and BeH_2 can be prepared by direct combination with hydrogen, however, the reaction must be carried out at extremely high pressures (9, 10). They can be readily synthesized by metathetical reactions involving an organo-metal derivative and lithium aluminum hydride, as shown in the following reaction



where M and R are the metal and organic radical respectively (11, 12).

Hydrogen compounds of elements belonging to Groups IVA, VA, VIA, VIIA and VIII are classified as the transitional metal hydrides. The hydrides formed by the metals in Groups IVA and VA can be formed by direct combination with hydrogen, and in many respects are quite similar to the ionic hydrides. The elements in Groups VIA, VIIA and VIII do not form true

stoichiometric compounds with hydrogen, but simply absorb large amounts of hydrogen in the lattice. Hydrogen can be assumed to be alloyed with the metal since it will, in certain cases, occupy definite positions in the metal lattice and not adversely change the properties of the metal.

The remaining metals belonging to Groups IB and IIB are classified as the borderline hydrides. These elements do not react with hydrogen to form compounds and exhibit only a limited amount of hydrogen solubility.

An attempt has been made to critically review the literature and to compile the thermal and thermodynamic data for these hydrides. An excellent compilation and evaluation of the dissociation pressure and the thermodynamic data for the hydrides of the alkali metals and the alkaline earth metals has been presented by Messer et al. (13). A general summary on the physical and chemical properties of the hydrides is given by Hurd (6). Other summaries on hydride data can be found in the following references (14, 15, 16, 17). Figure 1 is a plot of the temperature ($^{\circ}\text{K}$), at which the hydrides have a dissociation pressure or a vapor pressure equal to one atmosphere, as a function of the atomic number. Equations for the dissociation pressure of the solid hydrides which were used to calculate these temperatures, and the temperature range over which these data were experimentally determined are tabulated in Table 1. Similar data for the covalent hydrides are given

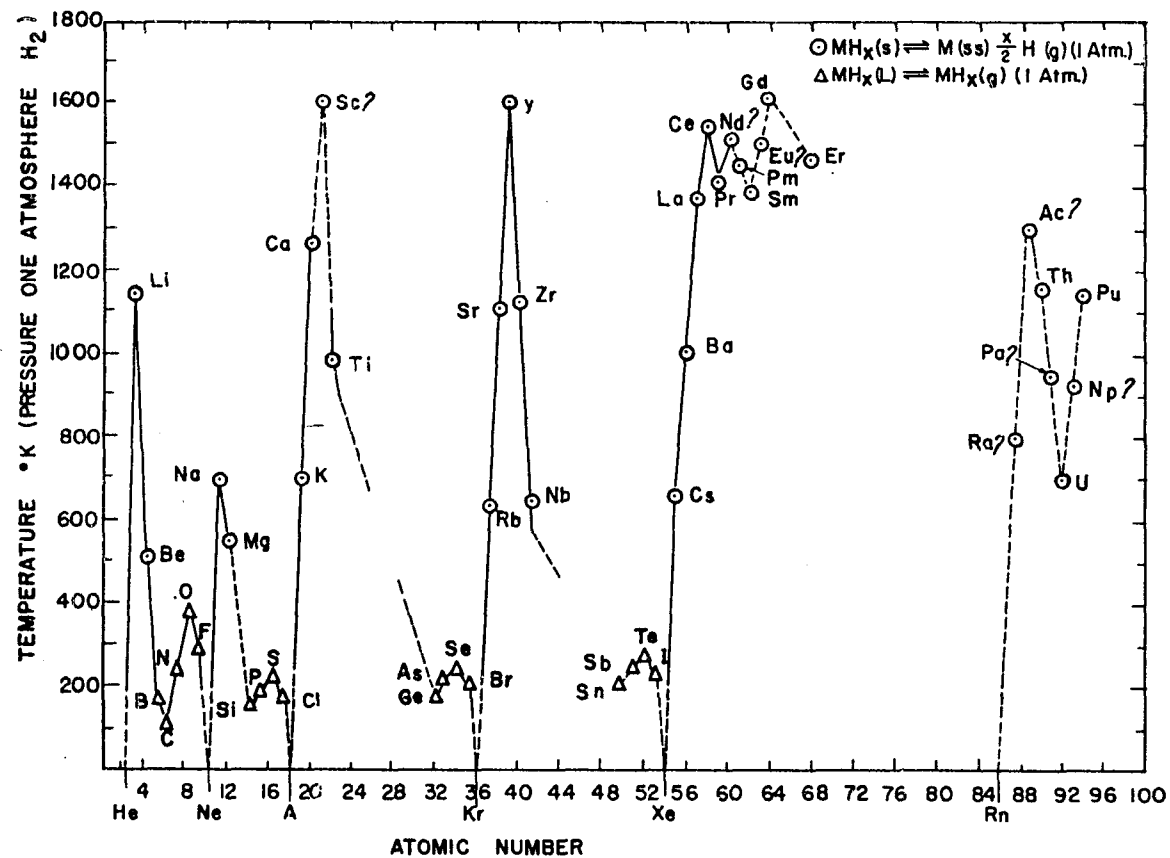


Figure 1. Temperature, as a function of atomic number, for which the dissociation pressure or the vapor pressure is equal to one atmosphere

Table 1. Equations for the dissociation pressure of solid hydrides

$$\log_{10} P_{H_2} = \frac{A}{T} + B + C \log_{10} T$$

Hydride	-A	B	C	Temperature range °C	Ref.
LiH	9337	11.131	-	770 - 825	13
NaH	6100	11.66	-	250 - 750	18
KH	6300	11.86	-	350 - 415	13
RbH	5680	11.80	-	250 - 350	19
CsH	5900	11.79	-	250 - 380	19
BeH ₂				Decomposes at 250°C	20
MgH ₂	3790	9.74	-	337 - 417	9, 10
CaH ₂	9840	10.70	-	780 - 860	21
CaH ₂	10870	11.493	-	636 - 892	22
SrH ₂	6500	8.66	-	1000 - 1100	23
BaH ₂	4000	6.86	-	500 - 1000	24
YH ₂	11058	9.82		650 - 800	25
LaH ₂	10858	10.758	-	150 - 800	26
CeH ₂	7417	7.708	-	150 - 800	26
PrH ₂	10446	10.229	-	150 - 800	26
NdH ₂	9796	9.370	-	150 - 800	26

MgH ₂	3790	9.74	-	337 - 417	9, 10
CaH ₂	9840	10.70	-	780 - 860	21
CaH ₂	10870	11.493	-	636 - 892	22
SrH ₂	6500	8.66	-	1000 - 1100	23
BaH ₂	4000	6.86	-	500 - 1000	24
YH ₂	11058	9.82		650 - 800	25
LaH ₂	10858	10.758	-	150 - 800	26
CeH ₂	7417	7.708	-	150 - 800	26
PrH ₂	10446	10.229	-	150 - 800	26
NdH ₂	9796	9.370	-	150 - 800	26
SmH ₂	11180	10.89	-	150 - 800	27
GdH ₂	10250	9.72	-	150 - 800	28
ErH ₂	11694	10.86	-	150 - 800	28
ThH ₂	7700	9.54	-	550 - 875	29
UH ₃	4590	9.39	-	300 - 450	30
PuH ₃	8165	10.01	-	400 - 800	31
TiH ₂	1063	1.806	-	175 - 1000	32
ZrH _{1.5}	11100	11.431	$2.94 \log \frac{x}{1.975-x}$	350 - 500	33, 34
NbH _{0.7}	4180	9.30		250 - 900	35

Table 2. Equations for the vapor pressure of covalent hydrides
 $\log_{10}P_{\text{mm}} = \frac{A}{T} + B + C \log_{10}T + DT$

Hydride	-A	B	-C	D	Ref.
CH ₄	559.6	13.038	2.514	-	36
NH ₃	1648.61	12.464	-	-0.0164	37
H ₂ O ^a				-	36
HF	1331	7.430	-	-	36
SiH ₄	645.9	6.881	-	-	36
PH ₃	797.8	7.180	-	-	36
SH ₂	1377	19.076	4.177	-	36
HCl	1158.5	17.080	3.534	-	36
GeH ₄	782.5	7.134	-	-	36
AsH ₃	1403.32	29.82835	9.43935	0.008037	38
SeH ₂	1067	7.482	-	-	36
HBr	1290	17.653	3.679	-	36
SnH ₄	966	7.257	-	-	36
SbH ₃	boiling point 256°K				6
TeH ₂	1235	7.441	-	-	36
HI	1456	17.740	3.764	-	36

$$^a \log_{10}P_{\text{mm}} = \frac{-2940}{T} + 1.207 + 3.86 \log_{10}T - 3.41 \times 10^{-3}T + 4.9 \times 10^{-8}T^2.$$

in Table 2. Data such as the dissociation pressure or the vapor pressure of the hydrides are of great utility because they must be taken into consideration in all practical applications of these compounds at high temperatures. They are also of importance because of the fundamental thermodynamic information which may be derived from them. Although the hydrides tabulated in Table 1 appear to form even stoichiometric compounds, most hydrides do not form even stoichiometric ratios, but approach this value. Consequently, the dissociation pressure equations are based on the so called "plateau" pressures obtained from isothermal plots of the equilibrium pressure as a function of the hydrogen to metal concentration. This represents the equilibrium of saturated solid solution of hydrogen in the metal and the metal hydride. As long as both phases are present, the pressure is essentially independent of the composition.

The dissociation reaction for the solid hydrides may be represented by the following reaction



which can be used to calculate the standard free energy of formation for the hydride. The equilibrium constant for the reaction can be expressed as

$$K = \frac{[\text{M}] [\text{H}_2]^{n/2}}{[\text{MH}_n]} \quad (2)$$

where $[M]$ and $[MH_2]$ are the activities of the metal and the hydride respectively, and $[H_2]$ is the equilibrium hydrogen pressure over the system. Assuming the activities of M and MH_n to be unity, the equilibrium constant reduces to $K = [P_{H_2}]^{n/2}$, and the standard free energy of dissociation ΔF° , can be calculated in Kcal/mol by

$$\Delta F^\circ = -RT \ln K = -n/2 \cdot 4.575T \log_{10} P_{H_2} \quad (3)$$

Substituting for $\log_{10} P_{H_2}$, the expression for the dissociation pressure for the hydride, one can calculate the standard free energy of dissociation of the hydride at the temperature in question. The reverse of equation 1 represents the formation of the hydride, therefore, the standard free energy of formation of the hydride can be obtained by changing the sign. The standard free energy of formation for the hydrides at 298° K are plotted in Figure 2 as a function of the atomic number. These values along with the temperature at which the dissociation pressure or the vapor pressure of the respective hydride is equal to one atmosphere are tabulated in Tables 3 and 4.

In some cases when no thermodynamic data was available for a particular hydride, the position of the element on the plot was estimated from the general trend for the adjacent hydrides. In such cases the plotted point is followed by a question mark and the curve to the point is drawn as a dashed line. It should also be noted that when more than one hydride

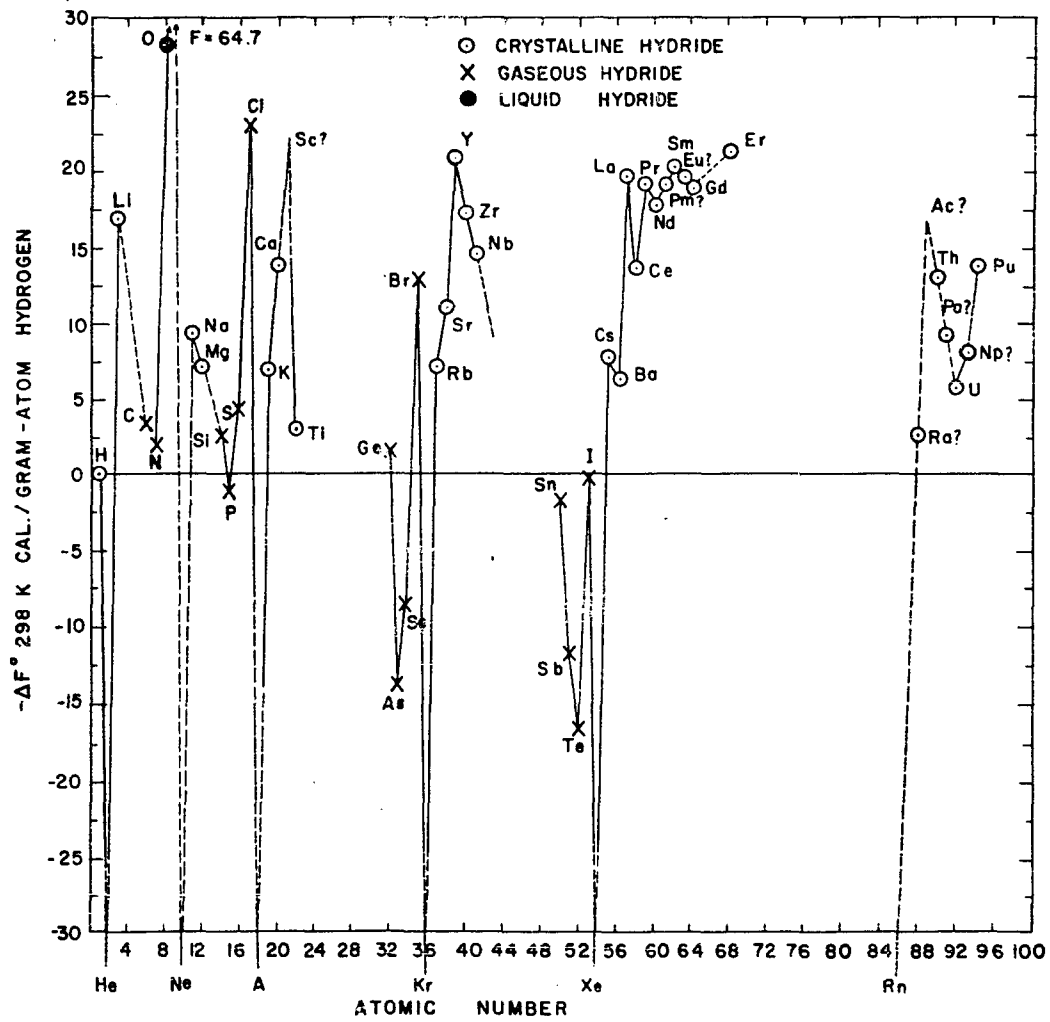


Figure 2. Standard free energy of formation for the hydrides as a function of atomic number

Table 3. Standard free energy of formation at 298°K for solid hydrides and the temperature at which the dissociation pressure is equal to one atmosphere hydrogen

Hydride	$-\Delta F^{\circ}_{298}$ Kcal/mol	Temperature (°K) ^a
LiH	15.74	1132
NaH	7.97	695
KH	13.63	701
RbH	6.99	637
CsH	7.42	662
MgH ₂	14.07	780
CaH ₂	27.16	1257
SrH ₂	21.86	1125
BaH ₂	12.88	1005
YH ₂	41.13	1594
LaH ₂	38.94	1378
CeH ₂	27.35	1537
PrH ₂	37.77	1422
NdH ₂	35.97	1510
SmH ₂	40.23	1396
GdH ₂	19.13	1620

MgH ₂	14.07	780
CaH ₂	27.16	1257
SrH ₂	21.86	1125
BaH ₂	12.88	1005
YH ₂	41.13	1594
LaH ₂	38.94	1378
CeH ₂	27.35	1537
PrH ₂	37.77	1422
NdH ₂	35.97	1510
SmH ₂	40.23	1396
GdH ₂	19.13	1620
ErH ₂	42.62	1466
ThH ₂	26.15	1156
UH ₃	17.70	705
PuH ₂	27.64	1145
TiH ₂	6.20	989
ZrH _{1.5}	25.64	1130
NbH _{0.7}	14.80	650 ^b

^aDissociation pressure equals one atmosphere hydrogen.

^bRepresents heat of solution.

Table 4. Standard free energy of formation at 298°K for gaseous or liquid hydrides and the temperature at which the vapor pressure is equal to one atmosphere hydrogen

Hydride	$-\Delta F^{\circ}_{298}$ Kcal/mol	Temperature (°K) ^a
CH ₄	12.14	110
NH ₃	3.98	240
H ₂ O	56.69	373
HF	64.70	298
SiH ₄	9.40	161
PH ₃	- 4.36	186
SH ₂	7.89	213
HCl	22.77	188
GeH ₄	6.00	183
AsH ₃	-41.60	208
SeH ₂	-17.00	232
HBr	12.72	206
SnH ₄	- 1.52	220
SbH ₃	-35.80	256
TeH ₂	-33.10	271
HI	- 0.31	243

^aDissociation pressure equals one atmosphere hydrogen.

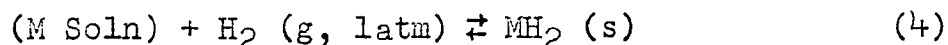
existed for a given element, such as carbon, data for the simplest hydride was plotted.

The plot of the standard free energy of formation of the hydrides as a function of the atomic number exhibits maxima at sodium, the Group IIIA elements, and at the beginning of the lanthanide and the actinide series. These hydrides also exhibit the largest degree of thermal stability as indicated by Figure 1. It is apparent that the metals which form the most stable hydrides are the more electropositive metals. Although no actual thermodynamic data was found for scandium or actinium, it is believed that these elements will occupy positions as shown on the plots. The majority of the hydrides, which form the most stable hydride compounds, can be prepared by reacting the elements with hydrogen gas at elevated temperatures and at a hydrogen pressure greater than the decomposition pressure of the hydride at the given temperature.

It is the purpose of this research to: (1) investigate the potential of separating solute impurities as hydrides from liquid metal solutions by hydrogen/liquid metal reactions, (2) to determine the degree to which these impurities can be removed as a function of temperature at one atmosphere hydrogen pressure and (3) to measure some of the thermodynamic relationships for the systems investigated.

In general the equilibrium reaction under consideration

may be written as



where M represents the solute of interest in a liquid metal solvent. The solute in the solvent reacts with hydrogen gas at one atmosphere pressure to give a solid hydride of essentially fixed composition, which separates from the solvent metal. The solvent metal under the experimental conditions is inert to hydrogen gas. The equilibrium constant may be expressed as

$$K = \frac{[MH_2]}{[H_2] [M]} = \frac{1}{[M]} \quad (5)$$

where MH_2 , the activity of the solid hydride, is taken as unity, $[M]$ is the activity of the solute in solution, and $[H_2]$ the activity of hydrogen which at one atmosphere pressure is taken as unity. Consequently the standard free energy of formation of the hydride, MH_2 , is related to the possible degree of separation by the equation

$$\begin{aligned} \Delta F^0_{(MH_2)} &= -RT \ln K = RT \ln [M] \\ &= RT \ln N + RT \ln \gamma \end{aligned} \quad (6)$$

where N is the equilibrium mole fraction of M in solution and γ the activity coefficient of M in solution relative to pure solid M.

If γ is one, or near one, then the larger the negative value for the standard free energy of formation of the hydride, the more complete the separation of the solute from the solvent.

However, for a given ΔF^0 value, the smaller the value for the activity coefficient, γ , or the greater the interaction of the solute with the solvent, the less favorable will be the precipitation of the solute.

The data on the metal hydrides given in Figures 1 and 2, show that the metals which form well defined crystalline hydrides with the largest standard free energy of formation, and also show the highest degree of thermal stability, are the more electropositive metals. Since a strong interaction between the solute and the solvent metal is undesirable, a solvent with about the same electronegativity value as the solutes to be separated would be desirable. The hydrides as compared to intermetallic compounds exhibit a greater decrease in stability with increasing temperature. Thus, the restrictions imposed on the liquid solvent are: (1) there should be little to no interaction between the solute and the solvent, (2) the solvent should be inert to hydrogen gas and (3) the solution should be low melting. Suitable elements which might be used as solvents are the elements belonging to Groups IIB, IIIB, Mg, Al, Sn, Pb, and Bi or eutectic mixtures of these metals. In the liquid state none of these elements react appreciably with hydrogen gas at one atmosphere pressure. The elements which form the more stable hydrides are the more electropositive elements, therefore, it would be advantageous to pick a solvent which is also electropositive

in character. From this point of view magnesium appears to be the most suitable solvent of the metals previously mentioned. Magnesium was the primary solvent used in these studies, however, hydrogen reactions were also studied using aluminum, zinc, and binary eutectic mixtures of these metals.

All of the reactions studied in this investigation were restricted to the formation and precipitation of the solid hydride from the liquid metal solution. Reactions involving the formation of gaseous hydrides were not considered. One of the aims of this study was to investigate hydrogen reactions for representative elements from Groups IIA, IIIA, IVA, the rare earth metals series, and the actinide metal series, with the hope of using these results as a basis to predict the behavior of the other elements in the respective group.

The precipitation of calcium, yttrium, lanthanum, cerium and thorium as the hydride from magnesium solutions with hydrogen at one atmosphere pressure was investigated. The precipitation of yttrium and thorium from magnesium - 55 wt. % zinc solution, and the precipitation of thorium and zirconium from an aluminum - 70 wt. % magnesium solution with hydrogen at one atmosphere pressure was also investigated.

The solubility of yttrium in liquid zinc and the solubility of zirconium in pure aluminum as a function of temperature was determined. Hydrogen equilibrations of these solutions were also investigated.

The binary phase diagrams for magnesium with calcium, cerium, thorium, lanthanum (39) and yttrium (40) have been determined. A low melting magnesium-rich eutectic solution is formed in each of these systems. Likewise they all form intermetallic compounds. Phase diagrams for the ternary systems which were investigated have not been determined.

Since the solute metals which are to be precipitated from the liquid metal solutions represent the more stable hydrides, and since these hydrides can be readily formed by direct combination with hydrogen gas, the separation of these solutes from the respective solvent seems feasible.

All of the reactions were investigated at one atmosphere hydrogen pressure as a function of temperature. From these data it is possible to determine the extent to which the solute metal can be precipitated from the solution, and an activity coefficient for the solute metal relative to either the solid or the liquid as the standard state at a given temperature can be calculated.

Reactions of this nature may be of interest in the re-processing of reactor fuels, or they may be used in the general purification of metals. A definite advantage of these reactions over the more common chlorination or oxidation reactions is that the precipitated hydride may be separated from the solvent by suitable means, such as filtration,

and the metal recovered simply by heating the hydride under reduced pressure to bring about the decomposition of the hydride.

II. APPARATUS

A. Vacuum System and Reactions Chamber

A schematic diagram of the apparatus used for the hydride equilibrations is shown in Figure 3. It consists of a vacuum system, a purification train, and a reaction chamber. The vacuum system is composed of a mechanical pump, a diffusion pump and a cold-trap. This was attached to the reaction chamber as pictured in Figure 3. A purification train, 6, was connected to the system. The purification train consisted of a one-inch stainless steel tube packed with uranium turnings, which was maintained at a temperature between 550°C to 600°C. In the purification of the hydrogen gas the uranium initially was converted to the hydride, however, upon heating to 600°C the hydride decomposes leaving the uranium as a finely divided powdered which has a large surface area to mass ratio and acts as an excellent purifying agent.

A detailed drawing of the reaction chamber is shown in Figure 4. The reaction chamber was constructed of standard 4-inch Schedule 40 seamless low-carbon steel pipe. This was sleeved with 1/8-inch 304 stainless steel tubing to protect the carbon steel from oxidizing at high temperatures. A water cooled brass flange was brazed to the top end of the reaction chamber. The charge was contained in a refractory crucible composed of MgO-15 wt. % MgF_2 . The crucible in turn was sleeved with a thin walled mild steel crucible, 12, in

Figure 4, to prevent the inside of the steel reaction chamber from coming in contact with the melt in case the refractory crucible developed a leak.

A sight glass, a thermocouple well, an outlet to a mercury manometer, a sampling tube and a vacuum couple for the stirring rod, as shown in Figure 4, was attached to the top brass cover plate. A vacuum seal was maintained between the two brass plates by means of a rubber "O" ring. The sampling chamber, 3, shown in Figure 4, was constructed of one-inch copper tubing which was silver brazed to a one-inch diameter ball vacuum seal valve, 6, which was attached to the brass cover plate. Two detachable vacuum couple seals, 2, were attached to the top of the one-inch copper tubing. This arrangement permitted samples of the liquid solution to be taken at temperature under a protective atmosphere without contaminating the solution with atmospheric gases.

The apparatus was equipped with a stirring paddle, 14, which was driven by a variable speed motor. The stirring paddle was fabricated from refractory material of the same composition as the crucible. The paddle consisted of a rectangular slab of refractory material which was 7 inches long, 1 1/4 inches wide, and 3/4 inch thick. This was attached to a 3/8-inch drill rod by a metal housing. Only the refractory portion of the stirrer came in contact with the liquid metal, when the solution was stirred.

Figure 3. Schematic diagram of system

- | | |
|---------------------------|------------------------------|
| 1a. 1-inch globe valve | 7. Uranium chips |
| 1b. 1-inch globe valve | 8. Fiber glass packing |
| 1c. 1-inch globe valve | 9. Hose cock |
| 2. Thermocouple gauge | 10. 1-inch ball vacuum valve |
| 3. Ionization gauge | 11. Vacuum couples |
| 4. Toggle valve | 12. Mercury manometer |
| 5. Red cap vacuum valve | 13. Cooling coils |
| 6. Gas purification train | |

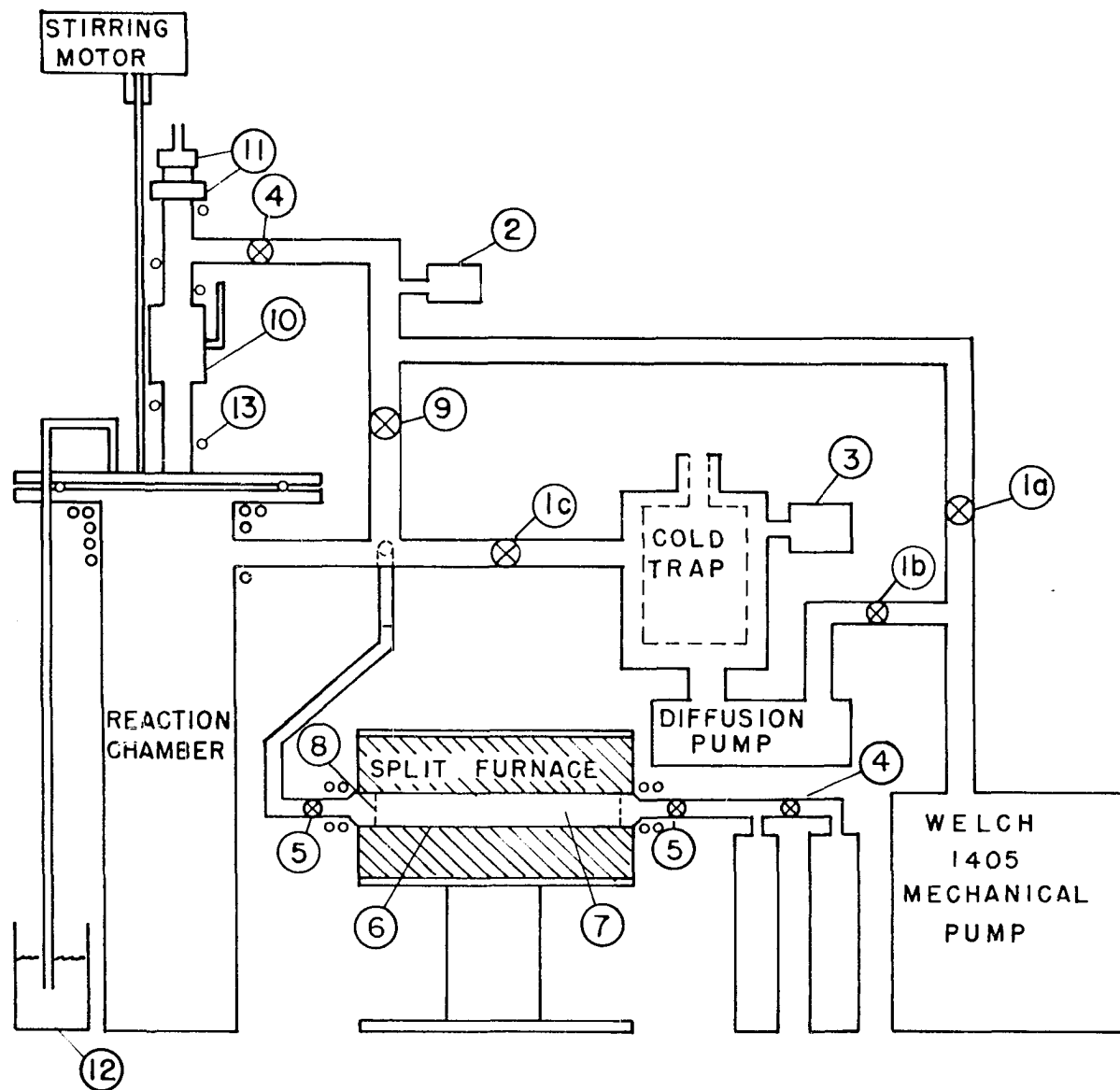
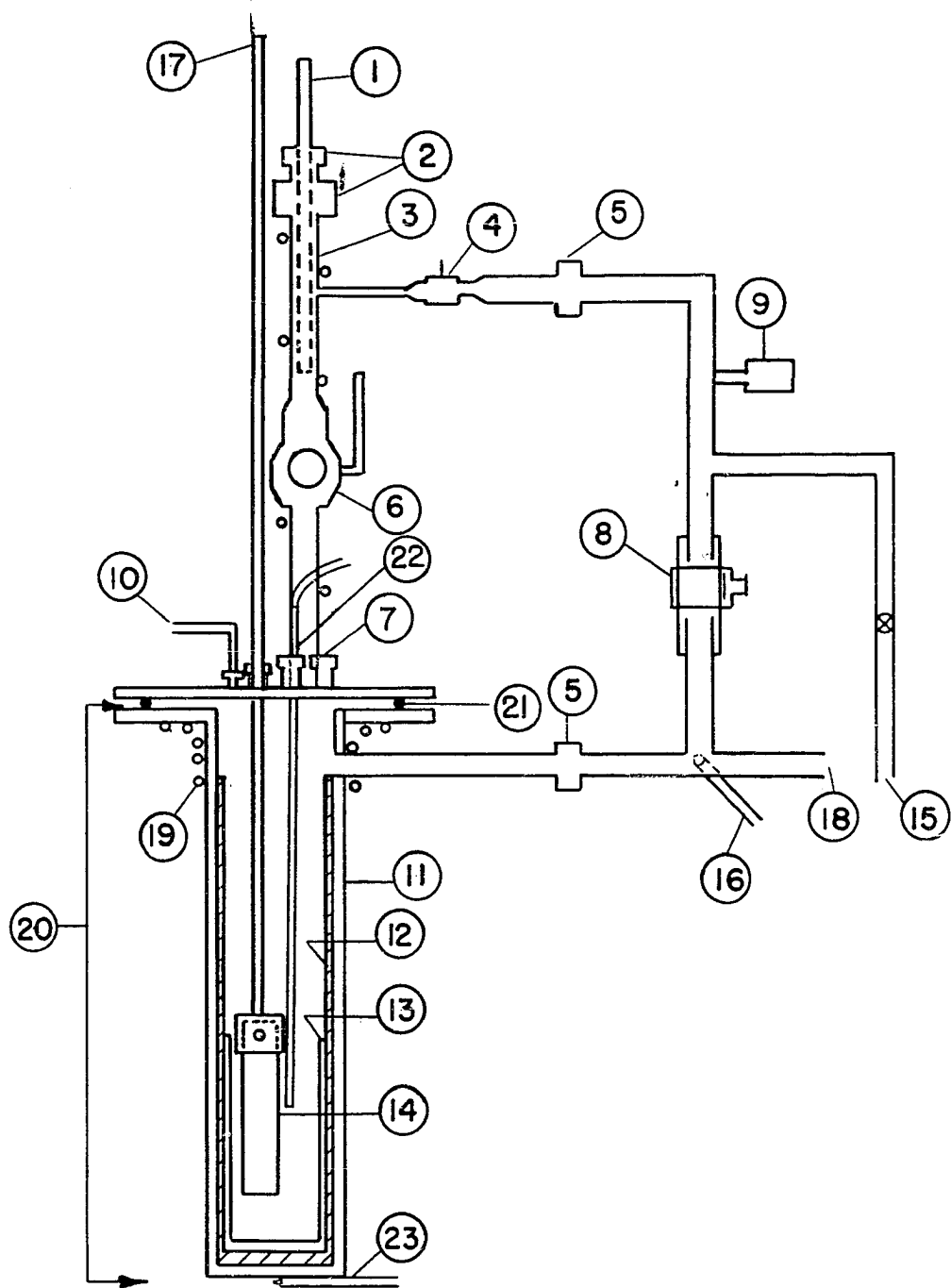


Figure 4. Reaction chamber

1. Sampling rod and holder
2. Vacuum seals
3. Sampling chamber
4. Toggle valve
5. Cenco vacuum couplings
6. 1-inch ball vacuum valve
7. Sight glass
8. Hose cock
9. Thermocouple gauge
10. To manometer
11. Carbon steel with stainless steel jacket
12. Carbon steel liner
13. $\text{MgO} - 15\% \text{MgF}_2$ crucible
14. $\text{MgO} - 15\% \text{MgF}_2$ stirrer
15. To vacuum pump
16. Gas inlet
17. Stirring rod to motor
18. To vacuum system
19. Cooling coils
20. Reaction chamber
21. Rubber "O" ring
22. Internal thermocouple used to measure temperature of the liquid solution
23. External thermocouple used to control furnace temperature



B. Sampling Devices

Samples of the liquid solution were obtained either by dipping or filtering. Schematic drawings of these sampling devices used are shown in Figure 5. The dipping device, A, consisted of a 1/4-inch steel rod, 5, attached to a tantalum holder, 7, which in turn contained a small refractory crucible, 4. This arrangement was used to dip a sample of the liquid solution simply by lowering the crucible into the liquid, and allowing the metal to flow into the crucible.

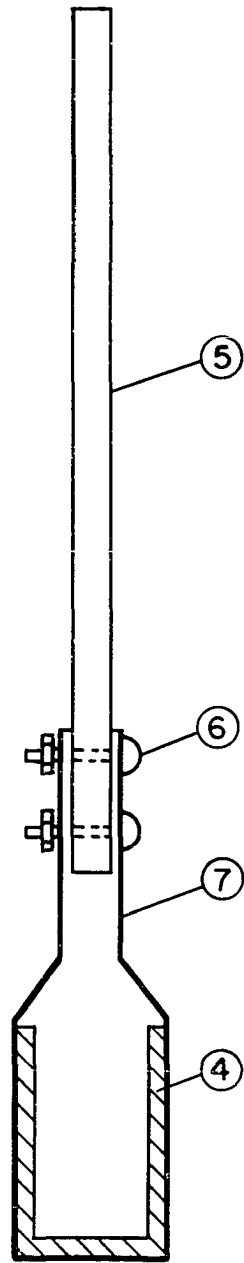
The filtering device, B, also shown in Figure 5, consisted of a 1/4-inch "OD" steel tube, 1, which was welded to a low carbon steel disk and this in turn was welded to a short piece of thin walled tantalum tubing. A porous refractory crucible was fitted into the short section of tantalum tubing and cemented-in with a water slurry of MgO. The water was removed from the MgO by baking in a furnace at 150°C for about 30 minutes. The MgO served to bond the crucible to the tantalum and also to plug up the space between the refractory crucible and the tantalum. A length of rubber tubing, not shown in the drawing, was attached to a vacuum pump. By pumping a partial vacuum on the steel tube, a small amount of the liquid metal solution was drawn into the crucible through the porous sides of the crucible.

Figure 5. Schematic diagram of sampling devices

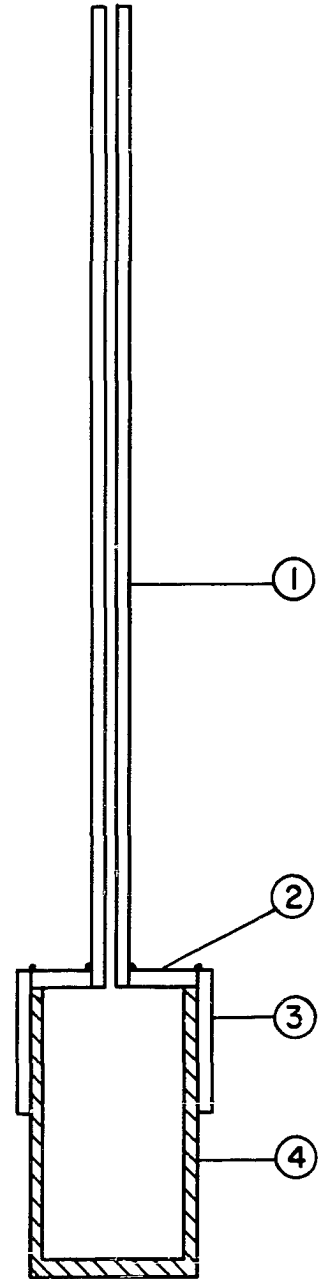
A. Dipping device

B. Filtering device

1. 1/4-inch steel tube
2. Steel disk welded to tantalum and steel tube
3. 30 mil tantalum tube
4. Porous MgO-crucible
5. 1/4-inch steel rod
6. Steel bolt
7. 10 mil tantalum holder



A



B

C. Furnace and Temperature Control

A 5-inch Kanthal wound resistance furnace was used to heat the reaction chamber. Temperatures were controlled to $\pm 2^{\circ}\text{C}$ by an automatic Honeywell Recorder and Controller. An alumel-chromel thermocouple 23, located on the exterior side at the bottom of the reaction chamber as shown in Figure 4, was used to control the temperature of the furnace. The actual temperature of the metal solution was obtained by an internal thermocouple immersed in the liquid solution. This temperature was measured with a Rubicon potentiometer. The thermocouple protection well consisted of a 3/8-inch steel tube which was welded shut at one end. This was sleeved with a thin walled tantalum tube to prevent the solution from coming in contact with the steel. The thermocouple well could be raised or lowered through a rubber "O" ring seal which made it possible to determine the temperature at any depth in the liquid metal solution.

III. EXPERIMENTAL

A. Materials

Metals used in this investigation include aluminum, calcium, cerium, magnesium, thorium, uranium, zirconium, zinc, and yttrium. The impurities present in these metals are listed in Table 5.

Bunker Hill zinc and electrolytic aluminum were used. The cerium, lanthanum, thorium, and yttrium metal was produced at this laboratory. Redistilled magnesium and calcium metal were used. The distillation of these metals was carried out at this laboratory from production grade material.

The helium gas used was 99.99% pure, the principal impurities being hydrogen and nitrogen. Hydrogen gas prior to its purification was 99.8% pure with moisture being the major impurity.

The refractory materials used in this investigation were fabricated at this laboratory. Magnesium oxide used to fabricate the crucibles and the stirring paddles contained the following impurities: 0.02 wt. % SiO_2 , 0.12 wt. % Fe_2O_3 , 0.25 wt. % Al_2O_3 , and 0.0015 wt. % B. Reagent grade magnesium fluoride was mixed with the magnesium oxide and the crucibles were fired at 1900°C . This produced impervious crucibles which were capable of containing the liquid metal solutions. The porous crucibles were produced in the same manner except in this case little or no MgF_2 was added to the magnesium oxide.

Table 5. Chemical analysis of materials

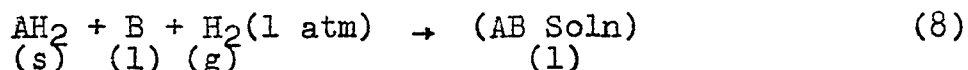
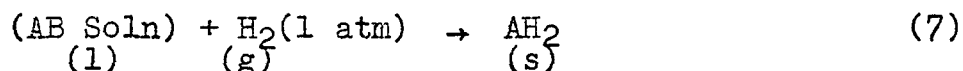
Material	%M	Concentration of impurities present in				
		C	N	O	Fe	Si
Mg	99.96+	250	45	30	40	tr
Al	99.99+	-	-	-	-	-
Ca	99.6 +	200	<100	-	tr	tr
Y	99.85+	200	<100	600-700	tr	-
La	99.1 +	100-300	100-300	100-300	1,000	250
Ce	99.4 +	100-300	100-300	100-300	800	250
Th	99.8 +	800	<100	100	800	<100
Zn	99.99+	-	-	-	30	-
Zr	99.94+	100	tr	tr	200	200
U	99.94+	200-400	-	-	35	-

ls

Concentration of impurities present in ppm quantities							
	O	Fe	Si	Mg	Ca	Nd	Others
45	30	40	tr	-	-	-	tr - Ca
-	-	-	-	-	-	-	
100	-	tr	tr	3,000	-	-	tr - Ba, Be
100	600-700	tr	-	<500	<10	-	tr - Ta
300	100-300	1,000	250	100	500	2,000	Pr - 300 Ce - 300 Ta - 1,000
300	100-300	800	250	600	500	200	La - 500 Pr - 500 Ta - 1,000
100	100	800	<100	<100	800	-	Mn < 100 B < 100 Cd < 100 Zn < 100 Be < 100
-	-	30	-	-	-	-	Pb - 30 Cd - 30
tr	tr	200	200	-	-	-	-
-	-	35	-	5	-	-	Mn - 100

B. Experimental Procedure

To determine the extent to which solute metal impurities can be separated as the hydride from the liquid metal solutions, the equilibrium was approached from two directions. This can be illustrated by the following reactions.



In reaction 7 the liquid metal solution was equilibrated with purified hydrogen gas at one atmosphere hydrogen pressure, whereas in reaction 8, the preformed hydride was equilibrated with the pure liquid solvent at one atmosphere pressure. Both of the reactions were carried out over the same temperature range. At equilibrium the results obtained for the two reactions should agree. This method of approach served as a check to assure that equilibrium conditions were obtained.

It is essential that the metals be adequately cleaned prior to melting and to insure that they do not become contaminated with surface oxide films due to outgassing of the system upon heating. The inside of the metal reaction chamber was cleaned by mechanical abrasion and then degreased with trichloroethylene. The metals were degreased in trichloroethylene and then either acid etched or in the case of the most reactive metals, mechanically abraded to remove

surface oxide films. The refractory crucible and the reaction chamber were thoroughly outgassed at elevated temperatures before making a run. The cleaned components (1,000 to 1,500 grams) were placed in the $\text{MgO} - 15 \text{ wt. } \% \text{MgF}_2$ crucible in the reaction chamber and the system was evacuated to less than one-tenth of a micron mercury pressure.

For reactions involving the equilibration of hydrogen with the liquid solution, the alloy initially was prepared under a purified helium atmosphere. After all of the solute metal had dissolved in the solvent, the solution was allowed to solidify, and the helium gas was pumped out. The system was flushed several times with hydrogen gas and subsequently heated under a hydrogen atmosphere. The hydrogen pressure in the system was controlled by allowing excess hydrogen gas to flow through the system into a mercury bubble trap. The exit tube was about one centimeter below the surface of the mercury. Thus the pressure over the system was maintained at a pressure of about one centimeter mercury in excess of atmospheric pressure. No attempt was made to determine the flow-rate, however, care was taken to assure a slow steady flow of gas at all times.

The purified hydrogen gas when brought in contact with the liquid metal solution preferentially reacts with the solute metal in the solution to form the respective hydride, which for all the systems studied, were solids over the temperature range investigated. The solution was stirred at 150 to 200 rpm in order to continually expose new surface

area of the liquid to the hydrogen gas to facilitate the attainment of equilibrium. Stirring also aided in eliminating thermal and concentration gradients in the liquid solution.

The apparatus was constructed so that a sample of the solution could be taken at temperature without exposing the melt to atmospheric gases. A small magnesia crucible (2 inches long with 1/2-inch outside diameter) held in a tantalum holder, which was attached to a 1/4-inch diameter steel rod as shown in Figure 5, was placed in the sampling chamber above the ball valve and the vacuum coupling screwed tight. The sampling chamber was evacuated by the mechanical pump by closing valve 1b located between the diffusion pump and the mechanical pump and opening valve 4 in the vacuum line to the sampling chamber, see Figure 3. After the chamber was evacuated, valve 1a was closed and purified gas was admitted by opening valve 9. The ball valve was then opened and the sampling device was lowered to the surface of the metal solution. It was left in this position for approximately 5 minutes to allow the crucible to reach the temperature of the surroundings before it was lowered into the melt. Care was taken not to stir the melt as the sample was taken. After the crucible was filled with liquid metal, it was drawn up into the water cooled sampling chamber. Here the sample was allowed to solidify and cool under the same atmosphere which

prevailed over the bath. The ball valve was closed as soon as the sample was pulled up into the sampling chamber. After the sample had cooled to room temperature, it was removed from the sampling chamber by unscrewing the vacuum seals, 2, shown in Figure 4. The sampling chamber was then reassembled for the next sample. Samples were taken on heating and cooling over the temperature range investigated.

A similar procedure was followed when a sample was filtered using the filtering device, B, shown in Figure 5. The device was lowered to the surface of the liquid and time was allowed for the crucible to reach the temperature of the surroundings. It was then lowered into the melt, allowing the melt to come in contact with only the crucible and the bottom end of the tantalum holder. A partial vacuum was pumped on the device drawing some of the liquid metal into the crucible through the porous walls of the crucible. The filtered sample was immediately pulled up into the water cooled chamber and allowed to cool. It was then removed as previously described and a new sampling device was inserted. It was found, that samples obtained by filtering gave more consistent results than did the samples obtained by dipping. This can be explained on the basis that upon dipping a sample variable amounts of suspended hydride were trapped in the sample.

A similar procedure was employed in studying reaction 8. The same precautions were taken to remove existing oxide

films on the metal and to clean the reaction chamber. In studying this reaction the system initially was evacuated, then flushed and filled with hydrogen gas prior to heating. The system was then heated to a temperature just below the melting point of the solvent metal and held at this temperature until the solute metal was converted to the hydride. The hydride reactions generally take place very rapidly and after no further reaction was noted, the temperature was raised to melt the solvent metal. The solution was then stirred and sampled over a given temperature range.

The solutions were stirred for approximately one hour at each temperature, and at least two samples were taken at each temperature. When the solution was sampled by dipping, the first sample was taken after the hydride was allowed to settle for 1/2 hour, and a second sample was taken 1/2 hour later. For the filtered samples the solution was allowed to settle for about 10 minutes prior to sampling.

C. Chemical Analysis

1. Determination of thorium in magnesium

The cylindrical samples taken from the liquid solutions were prepared for chemical analysis by machining off the exterior surface in a lathe. The machined samples were cut length-wise with a carborundum cut-off wheel into equal segments. Generally one segment was polished and microscopically examined to determine if the sample was homogenous, whereas

the remaining segment was used for analysis. In some cases the entire sample, after it had been cleaned and microscopically examined was used for analysis.

The analytical method employed in the determination of thorium was developed by Willard and Gordon (41). In this method the thorium was homogenously precipitated as thorium oxalate. A sample containing about 100 mg. of thorium was used. The sample was dissolved in concentrated nitric acid to which a small amount of fluosilicic acid was added to facilitate the dissolution of the sample. The thorium in the solution was precipitated as the oxalate upon the addition of methyl oxalate and a hot solution of oxalic acid. The solution was cooled to room temperature and filtered. The precipitate and filter paper, after it was thoroughly washed, was dried and ignited to thorium dioxide at 1000°C. The thorium was weighed as such and the % thorium calculated. Thorium, as analyzed by this method, yielded results with an accuracy of about 2 parts per thousand.

2. Determination of yttrium or lanthanum in magnesium

An analytical method developed by Fritz et al. (42) was used for the determination of yttrium in magnesium and for lanthanum in magnesium. In this method yttrium or lanthanum is titrated directly with ethylenediaminetetraacetic acid (hereafter referred to as EDTA) at a pH between 5.5 to 6.5 in the presence of magnesium. Arsenazo, [the trisodium salt of

3-(2 arsonaphenylazo) 4,5 - dihydroxy - 2,7 - naphthalene-disulfonic acid], was used as the indicator. Samples weighing between 2 to 4 grams were dissolved in dilute hydrochloric acid and diluted to 250 ml. Aliquots were taken so that they contained between 0.25 mmole to 1.0 mmole of yttrium or lanthanum. The solution was either evaporated or diluted to approximately 100 ml. 4 or 5 drops of pyridine were added, and the pH was adjusted to 5.5 with ammonium hydroxide or dilute hydrochloric acid. For solutions containing appreciable amounts of calcium or magnesium, the pH must be kept below 6.0, preferably at 5.5 or the hydroxides of the rare earths will precipitate. Adding about 5 ml of 0.1 M sulfosalicylic acid tends to act as a masking agent, and prevents the rare earth hydroxides from precipitating. Three to four drops of the indicator solution were added and the solution was titrated with 0.05 M EDTA solution taking the sharp violet to orange-red color change as the end point. Care was exercised to control and maintain the pH between 5.5 to 6.0 with a pH meter during the titration. The EDTA solution used in these titrations was standardized against standard solutions of zinc, yttrium and lanthanum using arsenazo as the indicator. The percent lanthanum or yttrium present in the sample was calculated by the relation

$$\%M = \frac{(N_{\text{EDTA}}) (\text{Vol. EDTA}) \text{ Factor Weight} \times 100\%}{\text{Wt. of Sample}},$$

where factor weights of 0.08892 and 0.01389 were used for the yttrium and the lanthanum respectively. Metals analyzed by this method yielded results with an accuracy of about 1 part per thousand.

3. Determination of yttrium in zinc and of yttrium in magnesium-zinc alloys

A similar procedure can be used for these analyses if the zinc is first extracted or removed from the solution. A standard anion exchange column was employed to remove the zinc from the solution. By passing the concentrated HCl solution through the column, the zinc remains on the column as the zinc chloride complex. The column was then washed with a dilute HCl solution to remove the remaining Y-Mg solution. The solutions were diluted to 500 ml, and aliquots were taken which were titrated for the amount of yttrium present using arsenazo as the indicator. These samples were also analyzed for the percent zinc present.

The zinc was removed from the anion exchange column by washing the column with distilled water. Aliquots of the solution were taken and about 50% by volume acetone was added. The pH was adjusted to 4.5 by adding ammonium acetate buffer solution. Several drops of dithiozone indicator solution were added and the solution was titrated to the pink to blue end point with EDTA. The results from these analyses are accurate to about 1 part per thousand.

4. Determination of cerium in magnesium

The analytical procedure used to determine cerium in magnesium was developed by Banks and O'Laughlin (43). Samples of the order of 4-6 grams were dissolved in hydrochloric acid. Approximately 5-10 ml of concentrated H_2SO_4 were added and the solution was heated until all of the HCl was liberated. The solution was diluted to approximately 250 ml with distilled water. Potassium peroxydisulfate was added to oxidize the cerium to the tetra-valent state. The solution was boiled vigorously for 20 minutes, cooled and a known excess of a standard ferrous ethylenediammonium sulfate solution was added. The excess ferrous solution was back titrated with a standard ceric sulfate solution. The per cent cerium was calculated by the following standard equation

$$\%Ce = \frac{(N_{FeII} V_{FeII} - N_{CeIV} V_{CeIV}) (.14013) \times 100}{\text{Sample Weight}}$$

Cerium analyzed by this method gave results with an estimated accuracy of about 2 parts per thousand.

5. Determination of calcium and zirconium

Calcium was determined in the presence of magnesium by a volumetric procedure developed by Diehl and Ellingboe (44). In this method the calcium was titrated in a strongly basic solution with EDTA using calcein as the indicator.

A volumetric procedure for the determination of zirconium using EDTA as described by Fritz and Johnson (45) was used to

analyze for the zirconium in the Zr-Al and the Zr-Al-Mg samples. Excess EDTA is added to the sample, forming a stable complex with the zirconium. The excess EDTA is then titrated with bismuth nitrate using thiourea as the indicator.

IV. EXPERIMENTAL RESULTS

One of the objectives of this investigation was to determine the extent to which solute impurities can be precipitated from liquid metal solvents with hydrogen. As was previously pointed out, representative elements from Groups IIA, IIIA, IVA, the rare earth metal series and the actinide series were investigated. For each system generally two equilibrations were made. One involved the reaction of the solution containing the solute with hydrogen at one atmosphere pressure, where the other involved the equilibration of the preformed solute hydride with the solvent at one atmosphere hydrogen pressure. In all of the equilibrations the solutions were stirred for one hour at each temperature setting. When samples were taken by the dipping method, the solution was allowed to settle for periods of a half and one hour respectively prior to taking the sample. For samples taken by the filtering method approximately five minutes was allowed for settling prior to sampling. Stirring and settling times of this magnitude were sufficient to obtain equilibrium. Generally two or three samples were taken at each temperature. The samples were taken on heating and cooling over a given temperature range. When no data were available on the solubility of the solute in the solvent solution, a solubility run was made to determine the solubility of the solute in the solvent. Comparing these

data with the data obtained from the hydride equilibrations, one can determine how effectively the hydrogen can reduce the solute concentration. Likewise if the phase diagram for the system under consideration has been determined, one can obtain an indication of the degree of separation of the solute from the solution, by comparing the results obtained from the hydrogen equilibrations with the concentrations specified by the liquidus of the phase diagram.

A. Hydride Reactions for Group IIA Elements

Calcium was the metal investigated for Group IIA metals. Magnesium-calcium solutions containing 16, 20, and 26 wt. % calcium were equilibrated with hydrogen gas at one atmosphere pressure. The phase diagram for the Ca-Mg system is given in Figure 6 (39). This system forms two eutectics, one which occurs at 16.2 wt. % calcium, and the other at 82 wt. % calcium which melt at 517°C and 445°C , respectively. An intermetallic compound, CaMg_2 , is formed at about 45 wt. % calcium, which melts congruently at 714°C . From the phase diagram it can be seen that the solutions used for the hydride equilibrations lie between the magnesium-rich eutectic and the compound.

Calcium combines directly with hydrogen gas to form the hydride CaH_2 . CaH_2 is classified as an ionic hydride and from the position of the hydride in Figures 1 and 2, it is apparent that it is one of the more stable hydride compounds.

The equilibration of Ca-Mg solutions with hydrogen gas were investigated over a temperature range of 625° to 900°C. Analytical results of the samples taken from these equilibrations are tabulated in Table 6. Figure 7 is a plot of the logarithm of the mole fraction of calcium in solution as a function of the reciprocal temperature in degrees Kelvin for the data tabulated in Table 6. A straight line relationship was observed and the equation for the line has been determined from a least squares treatment of the data. This equation and the equations to be determined in the following sections, will subsequently be tabulated in a table.

Although the precipitate was not identified by x-ray diffraction techniques, it was assumed that the decrease in calcium concentration of the Ca-Mg solution was brought about by the precipitation of calcium dihydride. From the concentration of calcium in magnesium as specified by the liquidus on the phase diagram, it is apparent that the decrease in calcium concentration was due to the hydrogen reaction. If no reaction would have been observed between the solution and the hydrogen gas, then the concentration of the calcium in the 16 wt. % solution would have remained constant upon cooling until the eutectic temperature was reached. Likewise upon cooling the 20 and 26 wt. % calcium solutions, the concentration would have remained constant until the liquidus line was reached. Analysis of the liquid solution indicated that the calcium concentration was below the concentration

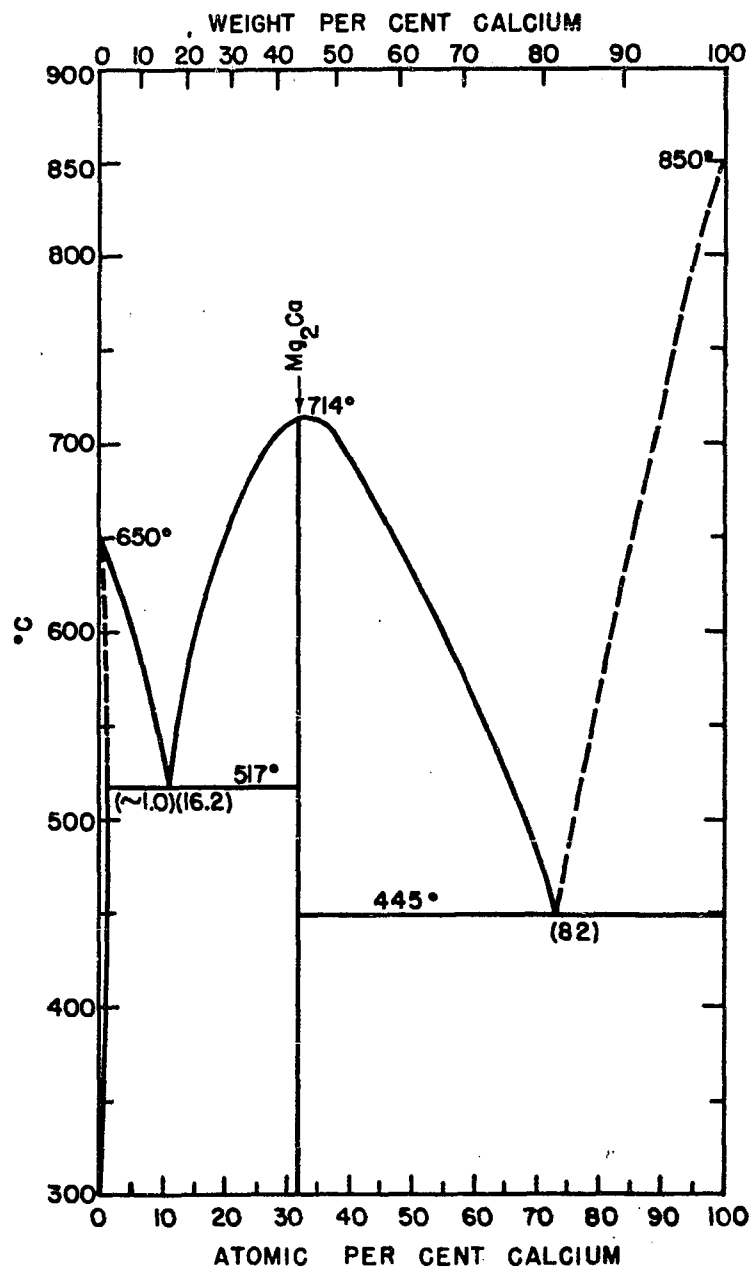


Figure 6. Magnesium-calcium phase diagram

Table 6. Analytical results for samples of the solution in which magnesium was equilibrated with CaH_2 at one atmosphere hydrogen pressure

Sample number	Temperature $^{\circ}\text{C}$	$10^4/T$ $^{\circ}\text{K}$	Wt. % calcium in the magnesium-rich phase	Mole fraction calcium in the magnesium-rich phase $\times 10^2$
PW5-200	625	11.13	6.95	4.34
194	670	10.60	10.59	6.85
211	675	10.55	9.74	6.15
212	675	10.55	10.66	6.75
361 ^a	696	10.32	11.26	7.15
201	700	10.28	12.61	8.10
200 ^a	700	10.28	12.37	7.80
208	736	9.975	14.49	9.30
202	775	9.55	16.90	11.00
203	775	9.55	18.43	12.00
207	830	9.075	21.50	14.00
366 ^a	844	8.95	21.58	14.30

^aFiltered samples.

specified by the liquidus curve for the phase diagram, but since the precipitate was not identified, it is possible that some complex $\text{Mg}_x\text{-Ca}_y\text{-H}_z$ compound could have been formed which precipitated from the solution. However, magnesium does not combine directly with hydrogen gas at these temperatures and

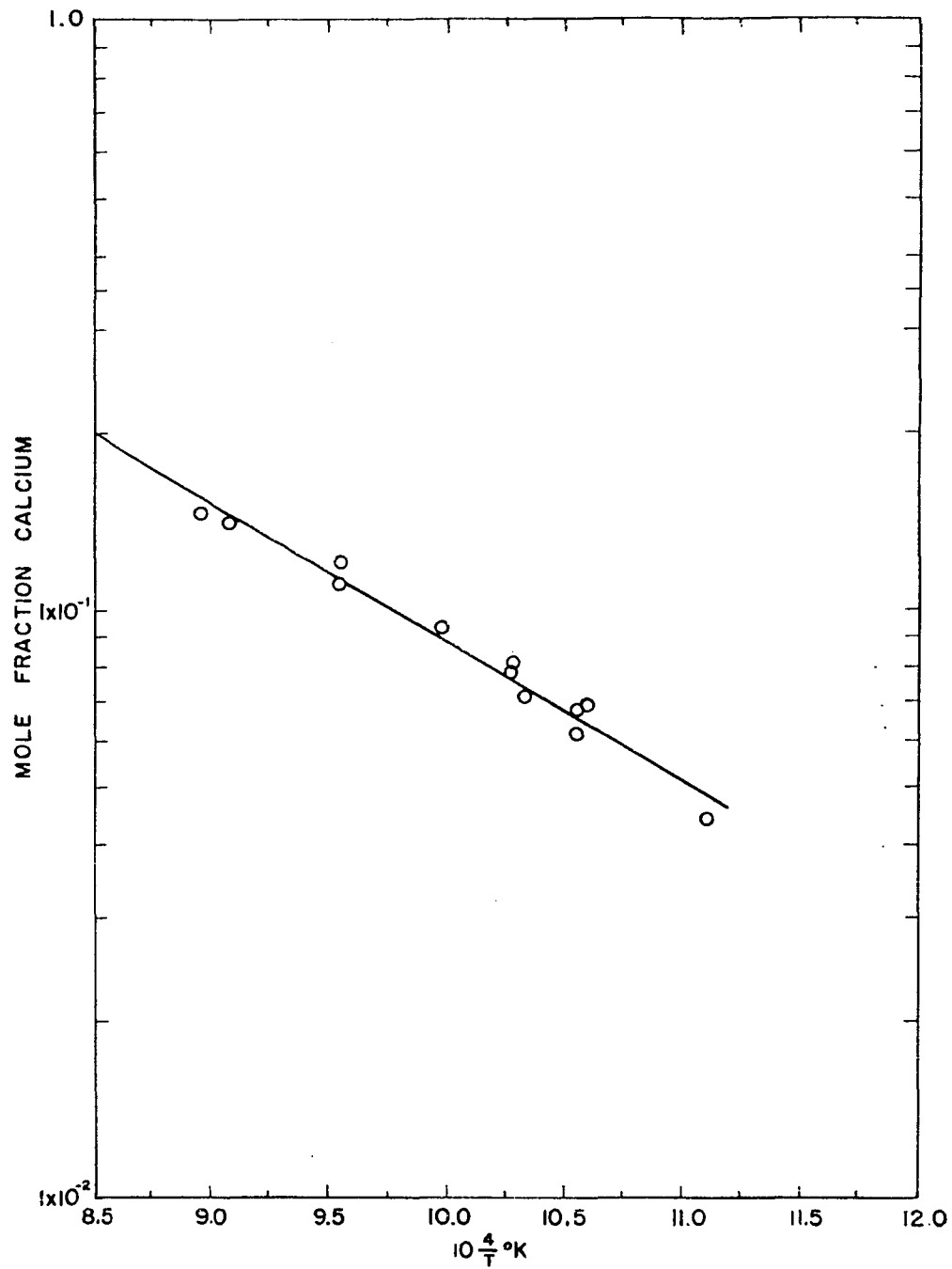


Figure 7. Mole fraction of calcium in the liquid phase as a function of temperature for CaH_2 equilibrated with magnesium at one atmosphere hydrogen pressure

pressures, thus it is not likely that such a species would be formed.

B. Hydride Reactions for Group IIIA Elements

Yttrium and lanthanum were the elements investigated from Group IIIA. The precipitation of yttrium as the hydride from three solvents, pure magnesium, magnesium - 55 wt. % zinc solution and pure zinc was investigated. Magnesium was the only solvent investigated for the lanthanum equilibrations.

The hydrides of yttrium and lanthanum can be formed by reacting the massive metals with hydrogen gas at an elevated temperature and at pressures greater than the dissociation pressures for the hydrides. Both of these metals form solid hydrides, which are quite stable compared to the rest of the metal hydrides. The phase diagram for the yttrium-magnesium system has been determined (40). Three compounds have been identified in this system, which occur at 21 wt. % magnesium, 41 wt. % magnesium, and 60 wt. % magnesium. All of these compounds decompose peritectically. A magnesium-rich eutectic is formed at 26 wt. % yttrium which melts at 567°C. Yttrium-magnesium solutions containing 26 wt. % yttrium, which is the eutectic composition, were equilibrated with hydrogen gas at one atmosphere pressure. Reactions in which preformed yttrium hydride was equilibrated with pure liquid magnesium at one atmosphere hydrogen pressure were also investigated.

Both of these reactions were investigated over a temperature range of 650° to 913°C. Samples of the liquid solution were obtained over this temperature range by dipping as well as by filtering. Analytical results obtained from these samples are listed in Tables 7 and 8. Data from these equilibrations are plotted in Figure 8, which is a plot of the logarithm of the mole fraction of yttrium in the magnesium-rich solution as a function of the reciprocal absolute temperature. Good agreement was obtained between the two reactions, thus it can be assumed that equilibrium was obtained.

Yttrium hydride was also equilibrated with a magnesium - 55 wt. % zinc solution at one atmosphere hydrogen pressure. The initial yttrium concentration was about 12.49 wt. %. This reaction was investigated over a temperature range of 485° to 850°C. It was possible to carry out the reaction at a lower temperature in this case since the Mg - 55 wt. % Zn solution represents a eutectic composition which melts at 343°C. Analytical results for the samples taken in these equilibrations are tabulated in Table 9, and a similar plot of the logarithm of the mole fraction of yttrium in the liquid phase as a function of the reciprocal absolute temperature is given in Figure 9. Equations of the lines drawn in Figures 8 and 9, and the probable error in the constants, have been determined by a least squares treatment. It can be seen from these data that yttrium is quite effectively

Table 7. Concentration of yttrium in magnesium-yttrium solution equilibrated with hydrogen at one atmosphere hydrogen pressure

Sample number	Temperature		Wt. % yttrium in magnesium-rich solution	Mole fraction yttrium in the magnesium-rich phase $\times 10^3$
	$^{\circ}\text{C}$	$10^4/T$ $^{\circ}\text{K}$		
PW5-237	670	10.60	0.262	0.719
249	670	10.60	0.270	0.730
239	700	10.28	0.327	0.894
240	700	10.28	0.233	0.698
253	700	10.28	0.320	0.880
254	700	10.28	0.460	1.04
256	754	9.74	1.07	2.09
257	754	9.75	0.74	2.03
241	765	9.63	0.96	2.65
242	765	9.63	0.94	2.60
234	805	9.28	2.23	6.20
243	805	9.28	2.81	7.74
236	851	8.89	5.56	15.80
258	851	8.89	6.68	19.20
259	851	8.89	5.10	14.50
247	913	8.44	11.83	35.40
248	913	8.44	11.33	33.80
321	833	9.04	3.49	9.78
322 ^a	833	9.04	3.16	8.84
324 ^a	769	9.60	1.09	3.02
325	760	10.33	0.96	2.65
326	715	10.12	0.33	0.877
327 ^a	708	10.19	0.34	0.926
328	708	10.19	0.34	0.926
329 ^a	662	10.70	0.14	0.382
330	660	10.71	0.19	0.511
331	653	10.80	0.11	0.292
332	728	9.98	0.50	0.137
335	793	9.38	1.84	5.10
336 ^a	800	9.32	1.88	5.20
337	860	8.82	5.09	14.40
338 ^a	868	8.76	4.11	11.60
339	863	8.80	5.80	16.60

^aFiltered samples.

Table 8. Concentration of yttrium in magnesium after equilibrations of yttrium hydride with pure magnesium at one atmosphere hydrogen pressure

Sample number	Temperature		Wt. % yttrium in the magnesium-rich phase	Mole fraction yttrium in the magnesium-rich phase $\times 10^3$
	$^{\circ}\text{C}$	$10^4/T$ $^{\circ}\text{K}$		
299	645	10.89	0.119	0.33
215	660	10.72	0.168	0.462
216	660	10.72	0.164	0.448
296	730	9.97	0.573	1.57
298	730	9.97	0.474	1.29
228	765	9.63	1.35	3.73
219	775	9.54	1.61	4.45
220	775	9.54	1.44	3.98
293	795	9.36	1.70	4.70
292	791	9.40	1.57	4.35
221	865	8.77	5.90	16.87
222	865	8.77	6.37	18.26
223	920	8.38	11.20	33.33

precipitated from these solutions at the lower temperatures investigated. The residual yttrium concentration in the yttrium-magnesium solution is about 0.19 wt. % at about 660°C , whereas about 2.5 wt. % yttrium is present in the Y-Mg-Zn solution at this temperature. However, by lowering the

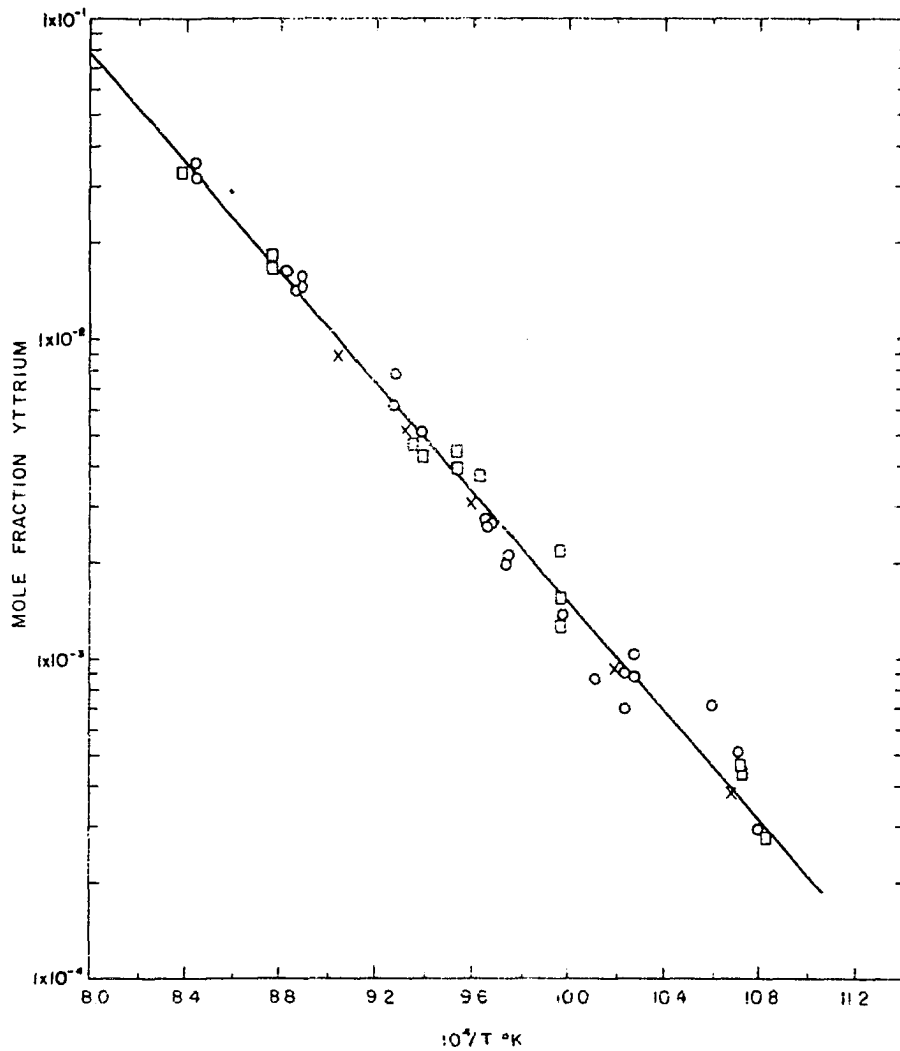


Figure 8. Mole fraction of yttrium in liquid magnesium as a function of temperature for equilibrations of YH_2 with magnesium (\square), and equilibrations of Mg-Y solutions with hydrogen [(\circ) dipped samples, (\times) filtered samples]

Table 9. Concentration of yttrium in Mg - 55 wt. % Zn solution after equilibration with YH_2 - initial yttrium concentration 12.49 wt. %

Sample number	Temperature		Analysis of liquid phase			Mole fraction yttrium $\times 10^3$	Method of sampling
	$^{\circ}\text{C}$	$10^4/\text{T } ^{\circ}\text{K}$	Wt. % Zn	Wt. % Mg	Wt. % Y		
PW5-357	490	13.11	53.77	46.06	0.19	0.787	Filtered
358	541	12.28	54.30	45.39	0.31	1.29	Dipped
359	565	11.93	53.58	45.97	0.65	2.69	Filtered
360	565	11.93	50.23	48.17	0.60	2.45	Dipped
355	608	11.35	53.42	45.28	1.30	5.42	Dipped
356	613	11.29	52.92	45.74	1.34	5.58	Filtered
346	668	10.63	52.27	45.22	2.51	10.40	Filtered
347	668	10.63	51.74	45.60	2.66	11.00	Dipped
348	710	10.17	51.46	43.84	4.70	20.00	Dipped
349	719	10.08	51.84	43.76	4.40	18.70	Filtered
351	758	9.70	48.36	42.09	9.55	41.70	Dipped
350	766	9.62	47.60	42.79	9.61	41.60	Filtered
354	795	9.36	47.90	39.72	12.38	55.60	Dipped
353	801	9.31	47.25	40.61	12.14	54.00	Dipped
352	810	9.24	47.73	40.46	11.81	52.60	Filtered

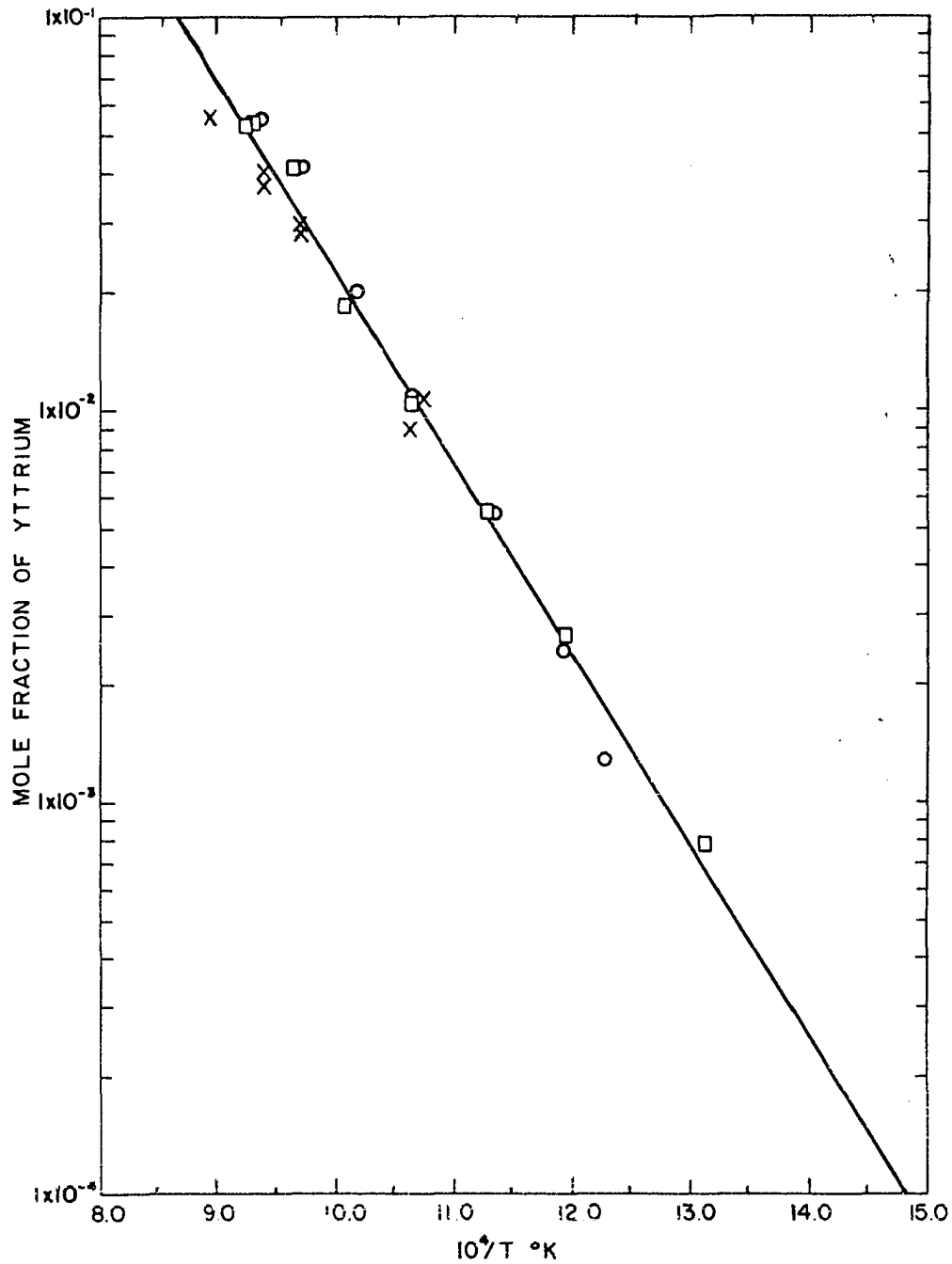


Figure 9. Mole fraction of yttrium in Mg - 55 wt. % Zn solution as a function of temperature for equilibrations with YH_2 [(O) dipped samples, (\square) filtered samples] and with yttrium and hydrogen [(X) dipped samples]

reaction temperature of the Y-Mg-Zn equilibration to 490°C , the residual yttrium concentration is reduced to 0.19 wt. %. Thus the same degree of separation can be achieved for the Y-Mg-Zn equilibrations if the reaction is carried out at a lower temperature.

The precipitated phase obtained from the Y-Mg and the Y-Mg-Zn equilibrations with hydrogen was identified by x-ray diffraction techniques to be yttrium dihydride. Yttrium dihydride is face-centered cubic with a lattice constant of 5.197 \AA (46). An x-ray diffraction pattern was taken on a Norelco diffractometer of a large crystallite of the hydride phase which was separated from the magnesium-yttrium solution. The observed "d" spacings, the calculated "d" spacings based on a lattice constant of 5.197 \AA , and the (hkl) reflections for the diffraction pattern are listed in Table 10. Three additional reflections were observed in addition to those given in Table 10. One of these reflections could be indexed as the (002) reflection for yttrium, whereas the other two reflections could not be indexed as reflections from the hydride, yttrium oxide or yttrium metal. These were low angle reflections and were probably extraneous reflections from the sample holder. An x-ray powder diffraction pattern of this same material was also taken with a Debye-Scherrer powder camera. It was possible to account for all of the first ten reflections for yttrium dihydride,

Table 10. X-ray diffractometer data for the precipitated phase taken from a Mg-Y solution, and Debye-Scherrer powder data for the precipitated phase taken from a Y-Mg-Zn solution after equilibration with hydrogen

hkl	d _{calc} (YH ₂)	d _{obs} (diffractometer)	d _{obs} (powder)
111	3.0004	3.0054	3.0079
200	2.5985	2.6048	2.6066
220	1.8374	1.8426	1.8424
311	1.5669	1.5690	1.5703
222	1.5002	1.5021	1.5032
400	1.2992	1.2995	1.3033
331	1.1922	1.1824	1.1952
420	1.1621	1.1636	1.1638
422	1.0608		1.0627
511, 333	1.0002		1.0051

and additional lines which were observed could be indexed as reflections for yttrium metal. The two low angle reflections observed on the diffractometer pattern were not observed on the powder pattern. This confirms the previous assumption that the two extraneous reflections observed in the diffractometer pattern were due to the sample holder.

A Debye-Scherrer powder pattern was also taken of the

precipitated material observed in Y-Mg-Zn solution, which had been equilibrated with hydrogen. The observed "d" spacings obtained from indexing this powder pattern are also listed in Table 10. For this pattern all of the observed reflections could be indexed as yttrium dihydride.

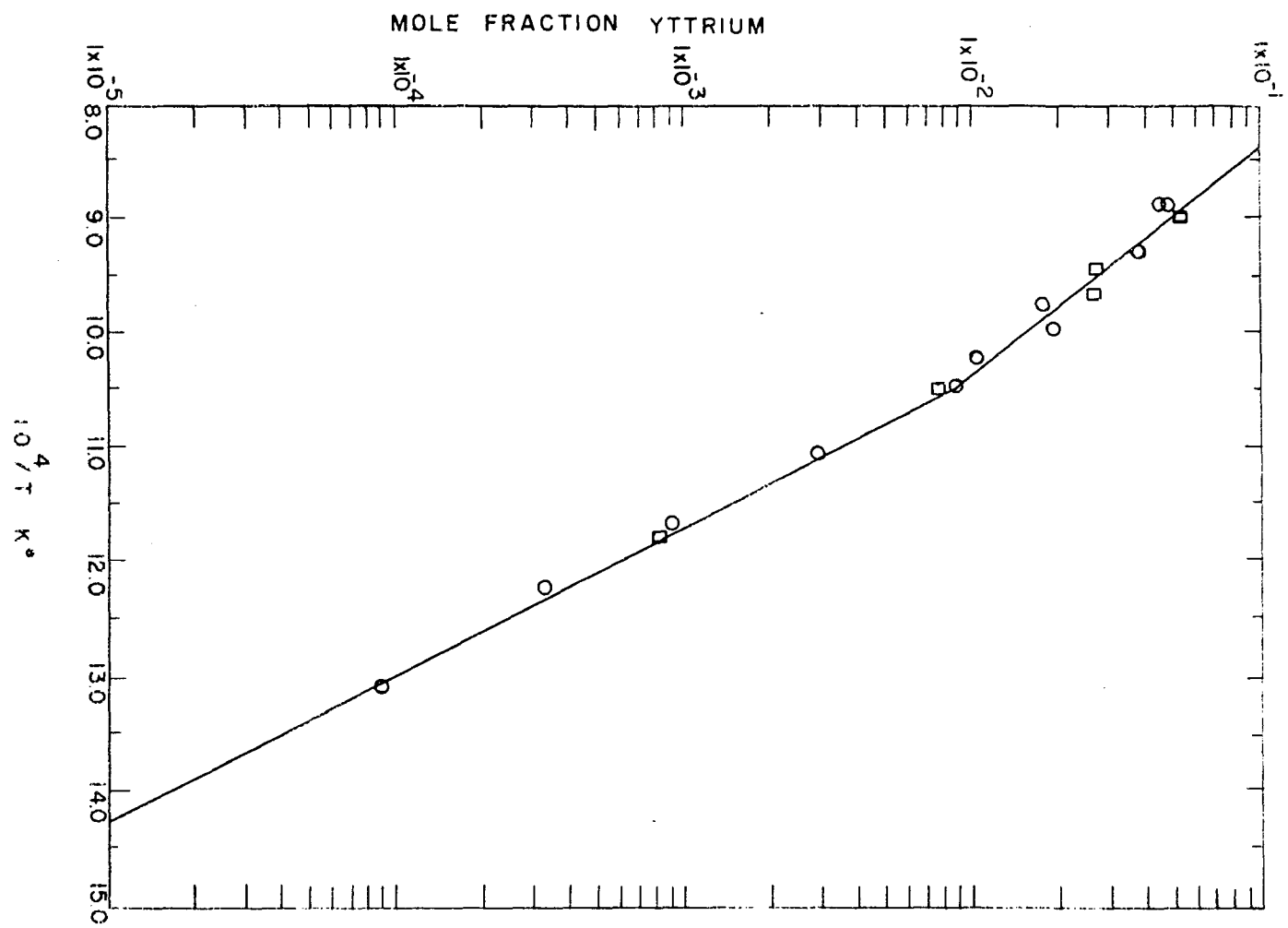
Therefore it can be concluded that yttrium was precipitated as yttrium dihydride from the yttrium-magnesium and the yttrium-magnesium-zinc solutions when equilibrated with hydrogen gas.

Since yttrium can be precipitated as the dihydride from pure magnesium and magnesium-zinc solutions, the possibilities of precipitating yttrium from liquid zinc was also investigated. The yttrium-zinc phase diagram has not been determined, consequently, in addition to the hydrogen equilibrations the solubility of yttrium in liquid zinc in the temperature range 494° to 851°C was determined. Two solubility experiments were made, one in which 2.0 wt. % yttrium (based on the weight of zinc used) was added to the charge and one in which 6.0 wt. % yttrium was added. These equilibrations were carried out under purified helium at one atmosphere pressure. Analytical data for the samples taken in these runs are tabulated in Table 11. A plot of the logarithm of the mole fraction of yttrium in the liquid solution as a function of the reciprocal absolute temperature is presented in Figure 10. A discontinuous change in the slope is observed at 685°C .

Table 11. Analytical results of samples taken after equilibration of liquid zinc with yttrium

Sample number	Temperature °C	$10^4/T$ °K	Wt. % yttrium in the zinc-rich phase	Mole fraction yttrium in the zinc-rich phase $\times 10^4$	Method of sampling
PW6-388	851	8.89	6.11	457.	Filtered
389	851	8.89	6.28	469.	Dipped
390	810	9.23	5.06	377.	Filtered
403	731	9.96	2.66	197.	Filtered
392	752	9.76	2.36	175.	Filtered
394	708	10.19	1.45	107.	Filtered
405	685	10.44	1.18	86.7	Filtered
461	634	11.03	0.404	29.0	Filtered
463	586	11.64	0.122	8.96	Filtered
464	547	12.19	0.044	3.26	Filtered
465	494	13.04	0.012	0.889	Filtered

Figure 10. Solubility of yttrium in zinc (○) under an atmosphere of helium and the solubility of yttrium in zinc (□) under an atmosphere of hydrogen as a function of temperature



Subsequent work by K. Gill (47) on the Y-Zn system has shown the existence of a peritectic horizontal at 685°C for zinc-rich alloys. Thermodynamic arguments can be used to show that this change in slope is due to the formation of a peritectic compound in the yttrium-zinc system. Equations, and the probable errors for the constants in the equations for the two straight line segments shown in Figure 10, have been determined by a least squares treatment.

To determine if yttrium can be separated as the hydride from yttrium-zinc solutions, liquid zinc was equilibrated with yttrium hydride at one atmosphere hydrogen pressure. The solutions initially contained 4 and 6 wt. % yttrium. These equilibrations were carried out over a temperature range of 845° to 579°C. Analytical results for the samples taken in these runs are tabulated in Table 12. These data are also plotted in Figure 10. From the data plotted in Figure 10, it is apparent that hydrogen at one atmosphere pressure does not appreciably affect the solubility of yttrium in liquid zinc.

The lanthanum-magnesium phase diagram consists of two eutectics, one at 11.2 wt. % lanthanum and the other at 90 wt. % lanthanum. Four intermediate phases Mg_9La (38.83 wt. % La), Mg_3La (65.57 wt. % La), MgLa (85.10 wt. % La), and MgLa_4 (95.81 wt. % La) are formed. (39) The magnesium-rich eutectic solution melts at 610°C. All of the compounds decompose peritectically except the Mg_3La , which has a

Table 12. Analytical results of samples taken after equilibration of YH_2 with liquid zinc at one atmosphere hydrogen pressure

Sample ^a number	Temperature		Wt. % yttrium in the zinc-rich phase	Mole fraction yttrium in the zinc-rich phase $\times 10^4$
	$^{\circ}\text{C}$	$10^4/T$ $^{\circ}\text{K}$		
PW6-395	845	8.91	7.035	527.
412	791	9.39	3.77	280.
400	764	9.64	3.59	266.
404	685	10.44	1.04	76.7
409	579	11.77	0.112	8.11

^aAll samples were filtered.

congruent melting point at 798°C .

Magnesium-lanthanum solutions containing 20, 28, and 45 wt. % lanthanum were equilibrated with hydrogen at one atmosphere pressure. In these equilibrations solid magnesium and lanthanum were held at 500°C in a hydrogen atmosphere until the lanthanum was completely converted to the hydride. The temperature was then raised to melt the magnesium, and the solution was stirred and sampled over a temperature range of 652° to 850°C . Analytical results for the residual lanthanum concentration in the liquid phase are tabulated in Table 13. A plot of the logarithm of the mole fraction of lanthanum in the solution as a function of the

Table 13. Concentration of lanthanum in magnesium solution equilibrated with hydrogen at one atmosphere hydrogen pressure

Sample number	Temperature °C	$10^4/T$ °K	Wt. % La in solution	Mole fraction La $\times 10^2$
442	842	8.97	46.71	0.133
447	784	9.46	36.34	9.08
451	760	9.63	33.85	8.22
445	752	9.75	31.73	7.52
446 ^a	753	9.75	31.36	7.40
458	748	9.80	28.82	6.62
454	733	9.94	26.66	5.98
452	725	10.02	26.35	5.89
450	721	10.06	26.40	5.91
449	721	10.06	25.81	5.75
453	702	10.26	22.58	4.86
456	701	10.27	22.30	4.78
455	691	10.38	20.76	4.40
459	673	10.57	17.80	3.65
457	657	10.75	14.46	2.87

^aSample dipped, all others were filtered.

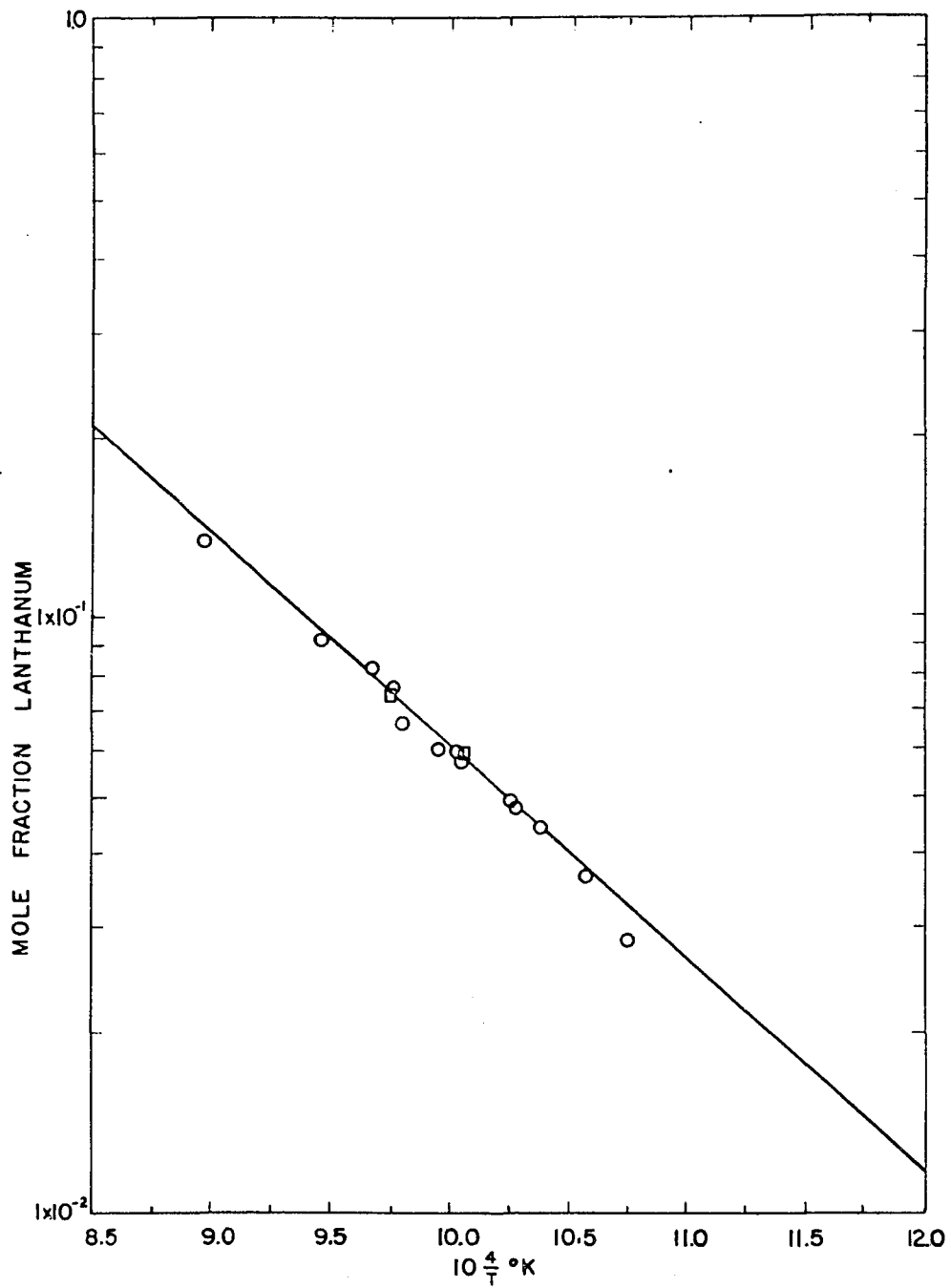


Figure 11. Mole fraction of lanthanum in liquid magnesium as a function of temperature of equilibrations of Mg-La solutions with hydrogen [(O) filtered samples, (□) dipped samples]

reciprocal temperature in degrees Kelvin is given in Figure 11.

Although the precipitated phase in the hydrogen-lanthanum-magnesium equilibrations was not identified by x-ray diffraction, it was assumed that the decrease in lanthanum concentration was due to the precipitation of lanthanum hydride.

C. Hydride Reactions for Group IVA Elements

Zirconium was chosen as the representative metal from Group IVA. Since the solubility of zirconium in liquid magnesium is very small, hydrogen equilibrations to separate the zirconium as the hydride from this solution were not studied.

The solubility of zirconium in liquid aluminum and the equilibration of zirconium hydride with liquid aluminum were determined. Analytical results are listed in Table 14. A plot of the logarithm of the mole fraction of zirconium in solution as a function of the reciprocal temperature in degrees Kelvin for these data is given in Figure 12. As can be seen from the plot, the solubility of zirconium in aluminum is not appreciably affected by hydrogen at one atmosphere pressure. Likewise, it was not possible to precipitate zirconium with hydrogen from U - 5.2 wt. % Cr solutions containing 2 to 4 wt. % zirconium at 900°C, or from Al - 70 wt. % Mg solutions containing 5 wt. % zirconium over a temperature range of 475° to 850°C at one atmosphere hydrogen

Table 14. Analytical results for the solubility of zirconium in liquid aluminum and for the equilibration of zirconium hydride with liquid aluminum at one atmosphere hydrogen pressure

Sample number	Temperature		Wt. % zirconium	Mole fraction zirconium $\times 10^3$	Method of sampling
	$^{\circ}\text{C}$	$10^4/T$ $^{\circ}\text{K}$			
PW5-74	666	10.65	0.11	0.325	Dipped ^a
63	673	10.57	0.12	0.355	Dipped ^b
65	730	9.97	0.19	0.562	Dipped ^a
62	750	9.78	0.28	0.830	Dipped ^b
66	754	9.74	0.34	1.02	Dipped ^a
61	795	9.36	0.37	1.10	Dipped ^b
68	805	9.28	0.40	1.187	Dipped ^a
69	815	9.19	0.496	1.473	Dipped ^a
60	830	9.066	0.52	1.542	Dipped ^b
70	853	8.88	0.54	1.605	Dipped ^a

^aZirconium hydride equilibration.

^bSolubility of zirconium in aluminum.

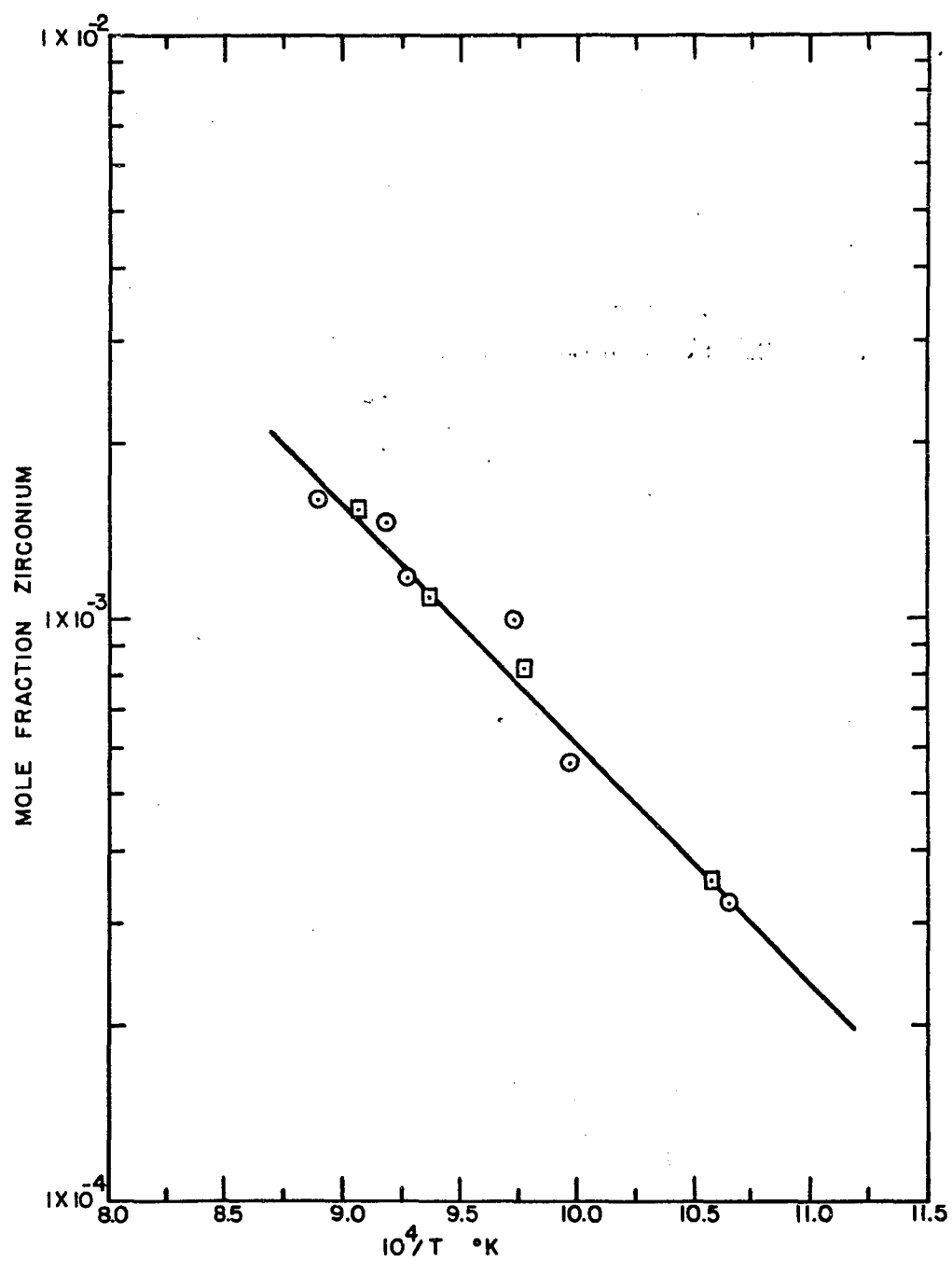


Figure 12. Mole fraction zirconium in liquid aluminum as a function of temperature [(\circ) solubility of zirconium in aluminum, (\square) zirconium hydride equilibrated with aluminum at one atmosphere hydrogen]

pressure. It was also not possible to separate zirconium from zinc-zirconium solutions with hydrogen at one atmosphere pressure.

D. Hydride Reactions for the Rare Earth Metals

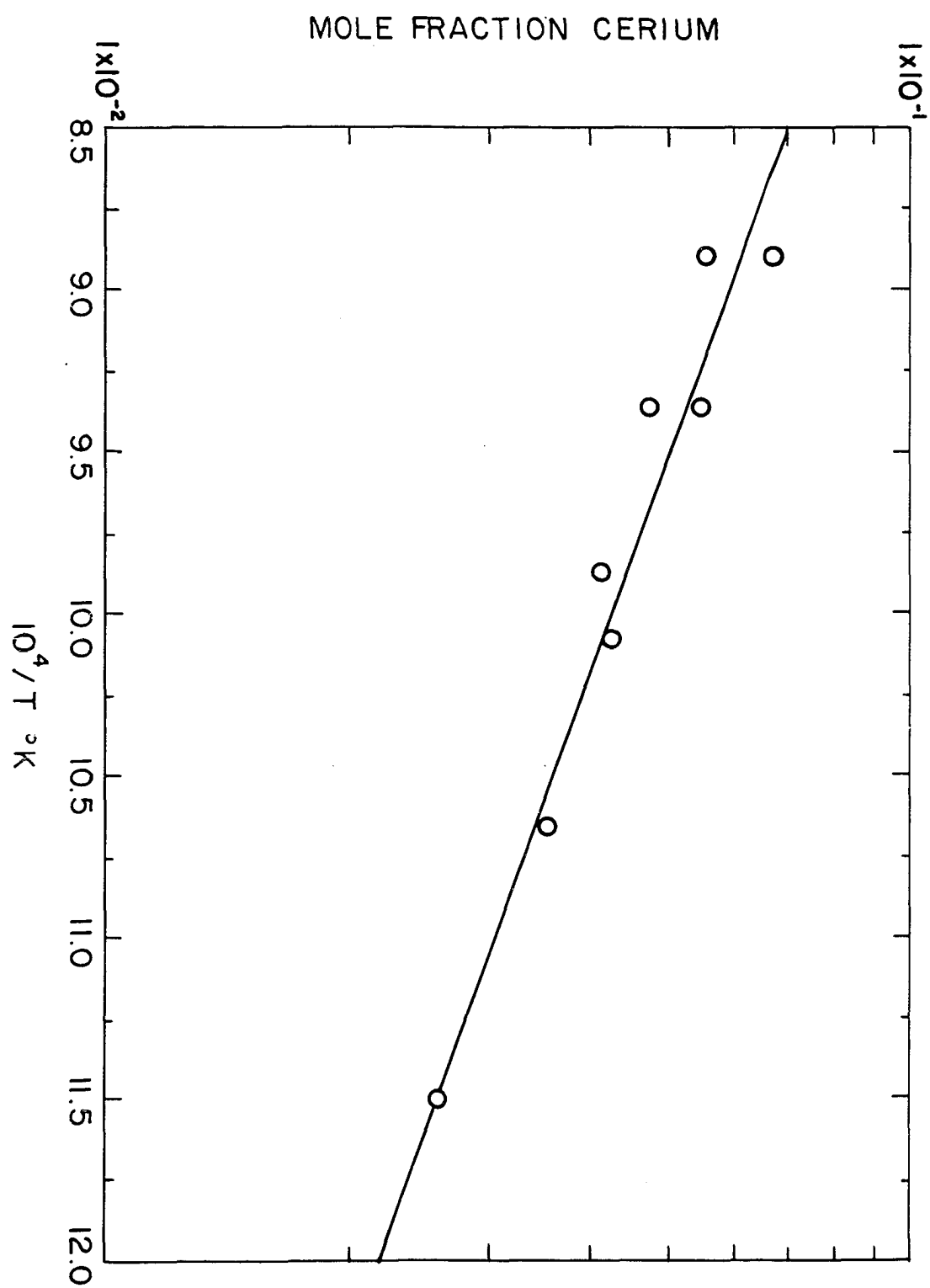
Cerium was chosen as the representative element for the rare earth metals. Four intermediate phases and two eutectics are formed in the cerium-magnesium system (39). All of the compounds except Mg_3Ce (65 wt. % Ce) decompose by a peritectic reaction. A low melting magnesium-rich eutectic is formed at 21 wt. % cerium with a melting temperature of 590°C . The phase diagram for the magnesium-cerium system is typical of the phase diagrams for the other rare earth metals with magnesium. Likewise the heats of formation for the compounds formed by the rare earth metals and magnesium are similar (48).

Magnesium-cerium solutions containing 30 wt. % cerium were equilibrated with hydrogen at one atmosphere pressure. These equilibrations were investigated over a temperature range of 597° to 850°C . Analytical results for the samples taken for these equilibrations are tabulated in Table 15. A plot of the logarithm of the mole fraction of cerium in the magnesium-rich solution as a function of the reciprocal temperature in degrees Kelvin is given in Figure 13. The least squares equation for the line drawn in Figure 13 has been determined.

Table 15. Concentration of cerium in magnesium-cerium solution equilibrated with hydrogen at one atmosphere hydrogen pressure

Sample number	Temperature °C $10^4/T$ °K	Wt. % cerium in magnesium-rich solution	Mole fraction cerium in magnesium-rich solution $\times 10^2$	Method of sampling
414	849 8.90	25.25	5.53	Filtered
413	849 8.90	29.40	6.70	Filtered
415	795 9.36	22.38	4.76	Filtered
416	795 9.36	24.98	5.46	Dipped
417	740 9.87	20.11	4.18	Filtered
421	712 10.15	20.33	4.24	Filtered
420	665 10.66	16.79	3.51	Filtered
4	597 11.50	13.32	2.60	Filtered

Figure 13. Mole fraction of cerium in liquid magnesium as a function of temperature at one atmosphere of hydrogen



E. Hydride Reactions for the Actinide Metals

Thorium was chosen as the representative element for the actinide series. The solubility of thorium and the precipitation of thorium as the hydride from magnesium - 55 wt. % zinc solutions as a function of temperature were investigated. The results for the solubility of thorium in the Mg - 55 wt. % Zn solution and the results for the concentration of thorium in the same solution equilibrated with hydrogen at one atmosphere pressure are tabulated in Tables 16 and 17 respectively. Data from both of these equilibrations are plotted in Figure 14. The horizontal segments of the lines in Figure 14 are due to the fact that the solution was not saturated with thorium over this temperature range. The concentration of thorium represented by the horizontal line for the solubility run was about 30 wt. % thorium, which represented the initial amount of thorium added. Similarly, the horizontal segment for the line for the hydrogen equilibrations represented about 23 wt. % thorium, which again represented the initial thorium concentration.

The results of a previous investigation (49) of the precipitation of thorium as the dihydride from thorium-magnesium solutions are also included in Figure 14 for comparison. From the data presented in Figure 14 it can be seen that by adding zinc to the thorium-magnesium solution, the amount of thorium removed as the hydride is greatly decreased,

Table 16. Analytical results for the solubility of thorium in magnesium - 55 wt. % zinc solution at one atmosphere helium pressure

Sample ^a number	Temperature		Wt. % Th	Analysis of liquid phase		
	°C	$10^4/T$ °K		Mole fraction Th $\times 10^2$	Wt. % Mg	Wt. % Zn
PW5-165	504	12.85	18.10	3.032	48.09	33.81
164	504	12.85	17.57	2.934	48.18	34.25
166	550	12.15	24.90	4.572	42.25	32.85
163	550	12.15	23.47	4.368	40.39	36.14
160	602	11.44	28.62	5.863	34.38	37.00
161	602	11.44	28.55	5.785	35.25	36.20
166	612	11.30	30.24	6.459	31.76	38.00

^aAll samples were dipped.

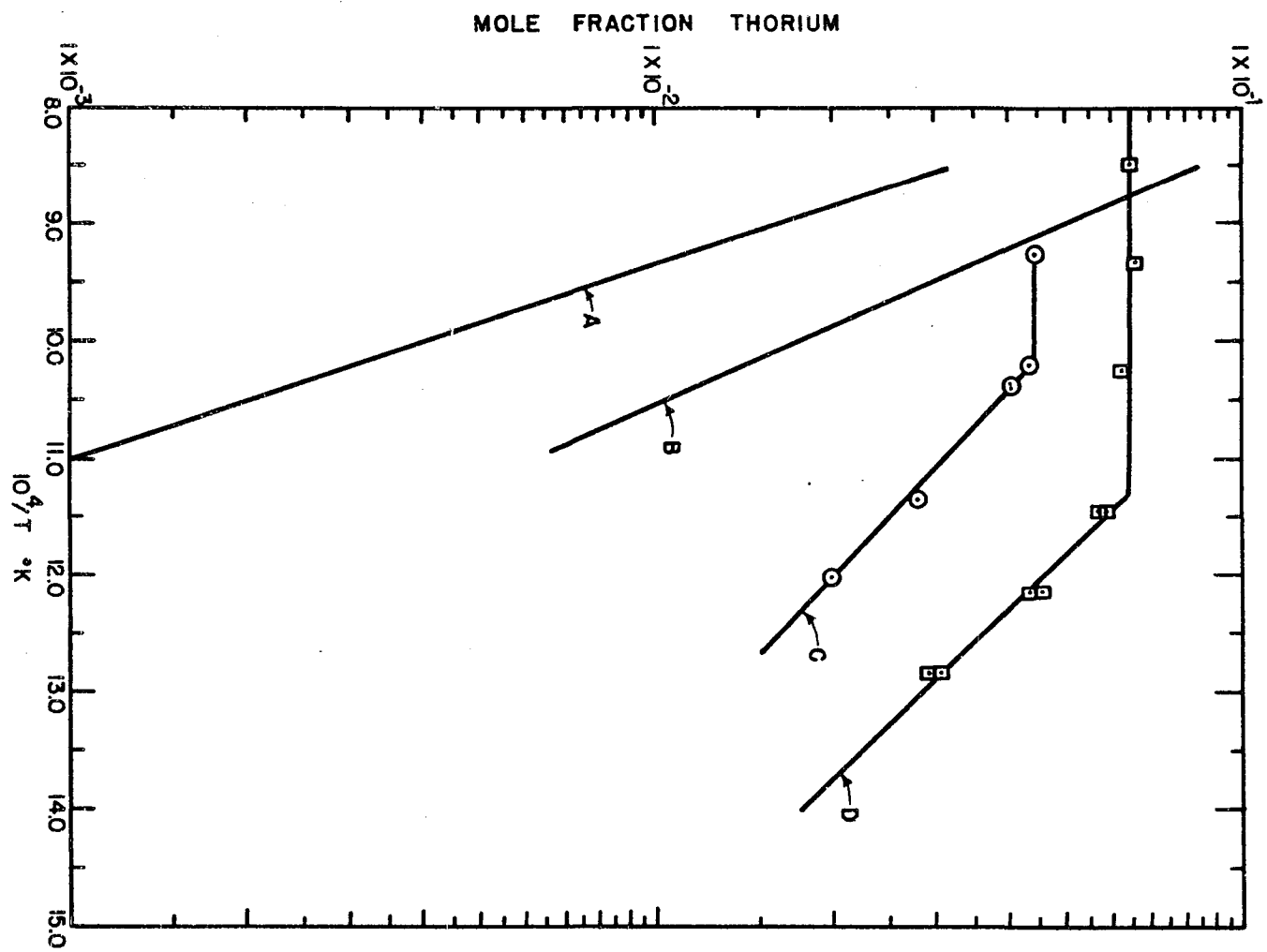
Table 17. Analytical results for the equilibration of thorium hydride with magnesium - 55 wt. % zinc solution at one atmosphere hydrogen pressure

Sample ^a number	Temperature		Analysis of liquid phase			
	°C	10 ⁴ /T °K	Wt. % Th	Mole fraction Th x10 ²	Wt. % Mg	Wt. % Zn
PW5-178	560	12.00	11.87	1.991	45.33	42.80
177	607	11.35	15.83	2.817	41.24	42.93
174	692	10.35	20.99	4.060	35.97	43.04
176	707	10.20	22.23	4.370	35.11	42.66
175	715	10.18	22.47	4.420	35.11	42.36

^aAll samples were dipped.

Figure 14. Mole fraction of thorium in solution as a function of temperature

- A. Solubility of thorium in liquid zinc
- B. Th-Mg solution equilibrated with one atmosphere hydrogen
- C. Th-Mg-Zn solution equilibrated with one atmosphere hydrogen
- D. Solubility of thorium in Mg - 55 wt. % Zn solution



which would indicate a strong interaction between the thorium and zinc atoms in the solution. Attempts were made to precipitate thorium as the hydride from thorium-zinc solutions at one atmosphere hydrogen pressure, however, no thorium was removed. This is consistent with the above results, which indicate that as the magnesium concentration is decreased, the amount of thorium precipitated as the hydride also decreases.

The solubility of thorium in magnesium - 70 wt. % aluminum solutions, and the precipitation of thorium as the hydride from these solutions were also investigated. Analytical results obtained for the solubility of thorium in the Mg-Al solutions are tabulated in Table 18. The results obtained from the hydrogen equilibrations are tabulated in Table 19. Plots of the logarithm of the mole fraction of thorium in the liquid phase as a function of the reciprocal temperature in degrees Kelvin for these solutions are presented in Figure 15.

Table 18. Analytical results for the solubility of thorium in Al - 70 wt. % Mg solutions at one atmosphere helium pressure

Sample ^a number	Temperature		Analysis of liquid phase			
	°C	$10^4/T$ °K	Wt. % Th	Mole fraction _L Th x 10^4	Wt. % Mg	Wt. % Al
PW5-12	797	9.37	0.701	7.602	71.30	27.999
14	755	9.72	0.575	6.227	67.50	31.925
17	730	9.90	0.514	5.586	65.80	33.686
16	702	10.28	0.320	3.470	69.30	30.380
18	607	11.37	0.135	1.470	64.30	35.565
47	558	12.03	0.093	1.011	65.15	34.757
19	508	12.80	0.063	0.681	64.60	35.337
49	486	13.16	0.038	0.411	69.60	30.362

^aAll samples were dipped.

Table 19. Analytical results for the equilibration of thorium hydride with Al - 70 wt. % Mg solutions at one atmosphere hydrogen pressure

Sample ^a number	Temperature		Analysis of liquid phase			
	°C	$10^4/T$ °K	Wt. % Th	Mole fraction Th $\times 10^4$	Wt. % Mg	Wt. % Al
PW5- 40	813	9.20	0.487	5.325	61.50	38.013
107	813	9.20	0.441	4.764	72.50	27.059
108	813	9.20	0.443	4.792	71.40	28.157
109	800	9.32	0.464	5.016	72.50	27.036
110	755	9.73	0.350	3.473	71.50	28.150
55	740	9.87	0.225	2.439	67.50	32.375
56	740	9.87	0.225	2.433	65.80	33.976
113	700	10.26	0.196	2.320	71.60	28.204
124	650	10.83	0.105	1.133	70.70	29.195
115	640	10.95	0.116	1.246	71.40	28.484
116	640	10.95	0.112	1.214	67.90	31.988
121	595	11.52	0.065	0.701	71.30	28.635
122	593	11.54	0.062	0.668	71.40	28.538
118	569	11.88	0.049	0.529	69.20	30.751
50	520	12.61	0.035	0.379	69.80	30.165
120	520	12.61	0.032	0.346	69.50	30.468
119	508	12.80	0.036	0.288	69.70	30.264

^aAll samples were dipped.

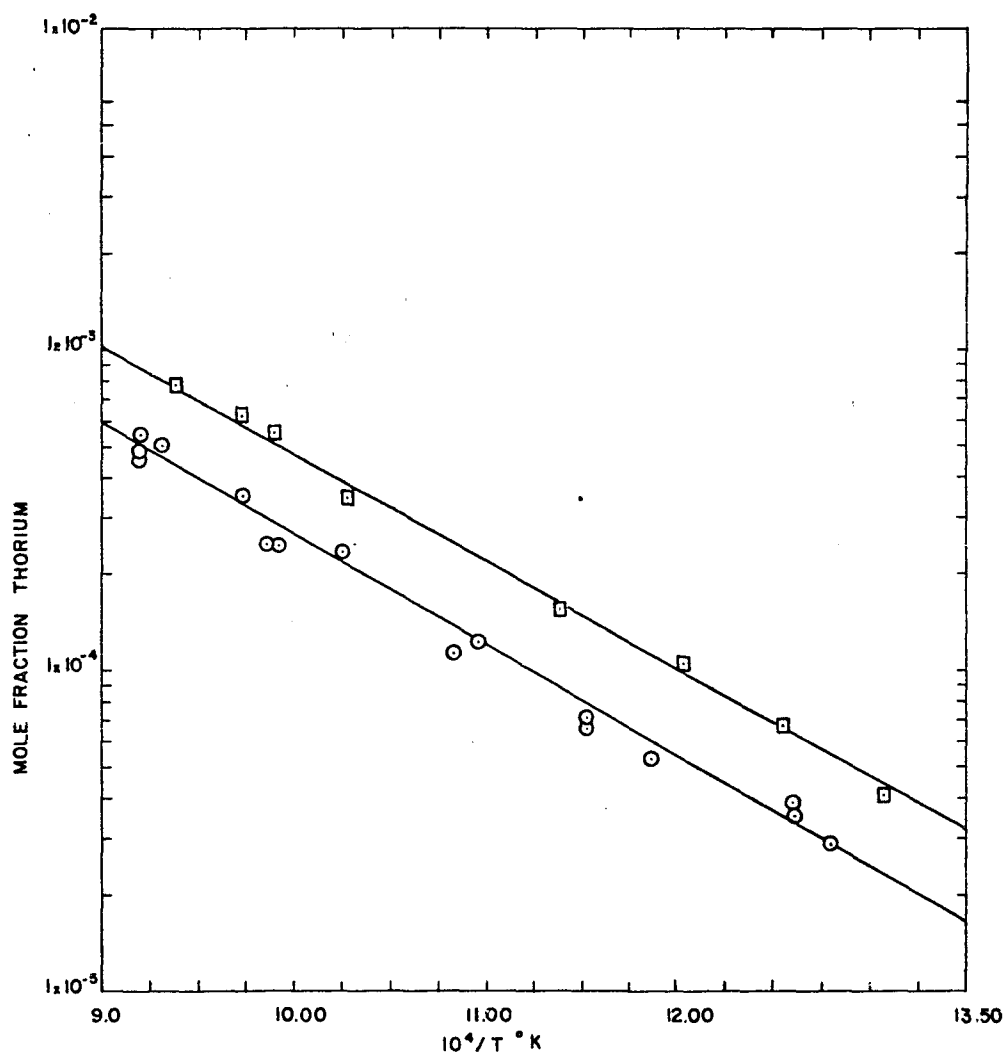
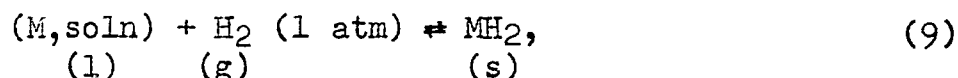


Figure 15. Mole fraction thorium in solution as a function of temperature [(□) solubility of thorium in Mg - 70 wt. % Al solution, (○) Th-Mg-Al solution equilibrated with hydrogen at one atmosphere pressure]

V. THERMODYNAMIC CALCULATIONS

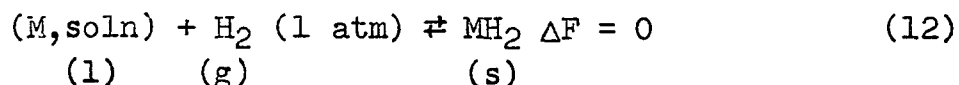
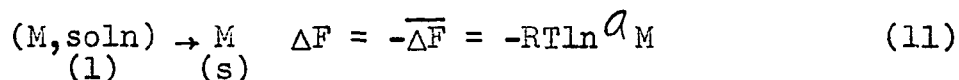
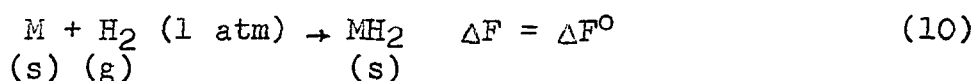
The activity coefficient for the solute metal (relative to the pure solid metal) in the liquid solvent can be calculated at a given temperature and composition from the experimentally determined mole fraction of the solute in solution. The activity coefficient of the solute with the pure liquid as the reference state can also be estimated.

The reaction studied in this research was the formation of the solid solute hydride from a liquid solution at one atmosphere hydrogen pressure. Assuming the formation of a solid hydride MH_2 , the reaction can be expressed as



where (M, soln) represents a liquid solution of fixed composition.

By combining the following two equations, one can arrive at the equilibrium reaction which was investigated



At equilibrium

$$\Delta F^0 = \overline{\Delta F} = RT \ln a_M = RT \ln N_M + RT \ln \gamma_M. \quad (13)$$

ΔF^0 , which is the standard free energy change for reaction 10 can be expressed as

$$\Delta F^0 = RT \ln P_{H_2}, \quad (14)$$

where P is the dissociation pressure for the solid hydride in question. The variation of the dissociation pressure with temperature for the hydride can normally be represented by the van't Hoff relation $\log_{10} P_{H_2} = \frac{-A}{T} + B$. The reverse of reaction 11 is the partial molar free energy of solution of solid M in a liquid solution, or it can be expressed as the free energy change which occurs when one gram-atom of solid M is dissolved in an infinitely large amount of solution (M) of a fixed composition. Combining equations 13 and 14 gives the following expression

$$\log_{10} \gamma_M = \log_{10} P_{H_2} - \log_{10} N, \quad (15)$$

where N_M and γ_M are respectively the mole fraction and activity coefficient of the solute metal in the solution equilibrated with hydrogen. The mole fraction of the solute in the respective solvent can be calculated at any temperature from the experimentally determined equations which are tabulated in Tables 20 and 21. Analytical expressions for the activity coefficient have been derived, and are tabulated in Table 22. The calculated activity coefficients at a given concentration for several temperatures are listed in Table 23.

By combining the following equations

Table 20. Least squares equations for residual solute concentration in various liquid metal solvents equilibrated with one atmosphere hydrogen:

$$\log_{10} N = \frac{-A \pm E_A}{T} + B \pm E_B$$

Solvent	Solute	A	Probable error in $A \pm E_A$	B	Probable error in $B \pm E_B$	Temperature range °C
Mg	Ca	2343	137	1.285	0.137	625 - 900
Mg	Y	8458	624	5.703	0.605	650 - 913
Mg - 55 wt. % Zn	Y	4857	134	3.199	0.140	485 - 850
Mg	La	3625	107	2.395	0.107	655 - 850
Mg	Ce	1376	137	0.0028	0.137	597 - 850
Mg	Th	4603	215	2.810	0.214	650 - 850
Mg - 55 wt. % Zn	Th	1880	30	0.558	0.0326	500 - 815
Mg - 70 wt. % Al	Th	3441	91	-0.152	0.098	500 - 815

Table 21. Equations for the solubility of various solutes in liquid metal solvents:

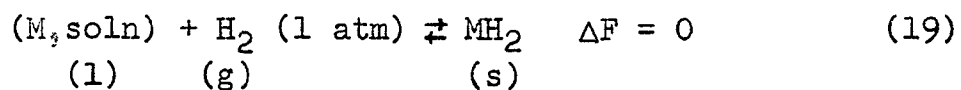
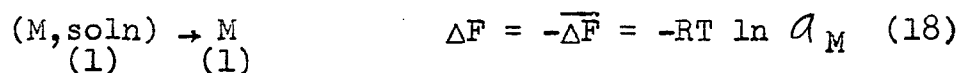
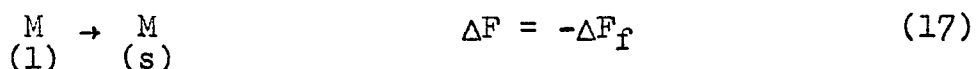
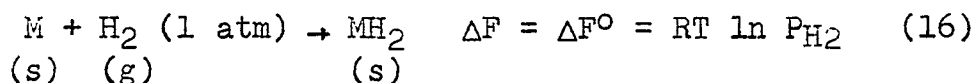
$$\log_{10} N = \frac{-A \pm E_A}{T} + B \pm E_B$$

Solvent	Solute	A	Probable error in $A \pm E_A$	B	Probable error in $B \pm E_B$	Temperature range °C	
Zn	Y	4769	348	2.946	0.332	685 - 850	
Zn	Y	7663	169	5.902	0.195	495 - 685	
Al	Zr	4089	316	0.896	0.305	650 - 850	
Al - 70 wt. % Mg	Th	3267	121	-0.056	0.134	500 - 815	∞
Mg - 55 wt. % Zn	Th	2067	156	1.144	0.187	500 - 815	

Table 22. Analytical expressions for the activity coefficient of various solutes in liquid solutions:

$$\log \gamma_A^s = \frac{-A}{T} + B$$

Solution	Solute	A	B
Ca-Mg	Ca	8526	7.327
Y-Mg	Y	2600	1.236
Y-Mg-Zn	Y	6201	3.740
La-Mg	La	7233	5.482
Ce-Mg	Ce	6041	4.824
Th-Mg	Th	3097	3.850
Th-Mg-Zn	Th	5820	6.102
Th-Mg-Al	Th	4259	6.812



it is possible to derive an analytical expression, whereby the activity coefficient for the solute metal in solution

Table 23. Calculated activity coefficient of the solute metal in the respective solution at a given temperature and composition using the solid as the standard state

Solution	Solute	Temperature °C					
		500	675	700	750	800	850
Ca-Mg	Ca, $N \times 10^2$	-	6.49	7.53	9.86	12.63	15.78
	γ_{Ca^s} , $\times 10^2$	-	2.15	3.27	9.84	24.10	54.3
Y-Mg	Y, $N \times 10^4$	-	7.60	10.24	27.23	66.13	148.0
	$\gamma_{Y^s} \times 10^2$	-	3.11	3.66	4.94	6.50	8.34
Y-Mg-Zn	Y, $N \times 10^3$	0.824	11.19	16.11	28.25	47.10	74.80
	$\gamma_{Y^s} \times 10^3$	0.052	1.58	2.33	4.76	9.14	16.50
La-Mg	La, $N \times 10^2$	-	3.72	4.67	7.11	10.39	14.69
	$\gamma_{La^s} \times 10^2$	-	0.711	1.12	2.58	6.93	10.96
Ce-Mg	Ce, $N \times 10^2$	-	3.56	3.84	4.55	5.25	5.99
	$\gamma_{Ce^s} \times 10^2$	-	2.83	4.12	8.30	15.63	27.86
Th-Mg	Th, $N \times 10^2$	-	0.902	1.20	2.05	3.16	5.14
	$\gamma_{Th^s} \times 1$	-	3.83	4.68	6.65	9.20	12.36
Th-Mg-Zn	Th, $N \times 10^2$	-	3.76	4.23	5.25	6.40	7.66
	$\gamma_{Th^s} \times 1$	-	0.918	1.32	2.58	4.76	8.32
Th-Mg-Al	Th, $N \times 10^4$	-	1.65	2.05	3.05	4.38	6.08
	$\gamma_{Th^s} \times 10^{-2}$	-	2.08	2.72	4.46	6.97	10.48

relative to the liquid state can be approximated. The free energy change for equation 16 was given by relation 14, and the free energy change for reaction 18 is the partial molar free energy of solution of liquid M in a liquid solution. In this case the free energy change for the melting of M, the solute metal, must be considered. If it is assumed that the difference in the heat capacity for solid and liquid M can be neglected, the free energy change for reaction 17 can be expressed as

$$\Delta F_f = \Delta H_f \left[1 - \frac{T}{T_m} \right],$$

where ΔH_f is the heat of fusion and T_m is the melting temperature of M expressed in degrees Kelvin. At equilibrium ΔF_{19} is zero and $\overline{\Delta F} = \Delta F^0 - \Delta F_f$, which yields

$$\log \gamma_M = -\log_{10} N_M + \log_{10} P_{H_2} - \frac{\Delta F_f}{RT}. \quad (20)$$

By substituting the experimentally determined expression for $\log_{10} H$, the dissociation pressure expression for $\log_{10} P_{H_2}$ for the hydride and the free energy of fusion at the temperature in question, it is possible to use equation 20 to approximate the activity coefficient of M in solution relative to the liquid state. For metals which are normally liquids at the temperature in question, the reference state is the pure liquid. However, for a metal whose melting temperature is above the temperature in question, the reference state is super cooled liquid, a hypothetical reference state.

Table 24. The per cent solute precipitated by hydrogen from the saturated solvent at 700°C

Solute	Solvent	% precipitated
Ca	Mg	73.1
Ce	Mg	73.9
La	Mg	52.8
Y	Mg	99.99
Th	Mg	85.0
Th	Mg-Zn	59.8
Th	Mg-Al	51.2

The per cent of solute precipitated by the hydrogen gas from each saturated solvent at 700°C is tabulated in Table 24. These values are based on the solute concentration obtained from the liquidus curve of the equilibrium phase diagram or from a solubility equation determined in this investigation. It was not possible to calculate the per cent yttrium precipitated from a Mg-Zn-Y solution, since the saturation solubility of yttrium in the solution is not known.

VI. DISCUSSION OF RESULTS

The least squares solubility curves for the hydride equilibrations, with the exception of the curves for the Mg-Zn-Th and the Mg-Al-Th systems, are presented in Figure 16. At a given temperature, for example 727°C , $\frac{10^4}{T} = 10.00$, for the systems employing pure magnesium as the solvent, it can be seen that the residual solute content is least for the Mg-Y system and greatest for the Mg-Ca system. In all systems the residual solute concentration decreases as the reaction temperature is lowered, indicating that for reactions of this nature low melting solvents are desirable.

The percent of solute precipitated from the saturated solvent by hydrogen at 700°C and one atmosphere pressure was given for the various solvents in Table 24. Calcium was the only metal investigated from Group IIA, and as can be seen from the data in Table 24, about 73% of the calcium is precipitated from a saturated solution. Yttrium and lanthanum were investigated from Group IIIA, and it was possible to precipitate 99.99% of the yttrium as the hydride from a saturated Y-Mg solution, whereas only 52.8% of the lanthanum is precipitated from a saturated La-Mg solution. Cerium was the metal studied from the rare earth metal series, and about 74% of the metal is precipitated from the Mg-Ce solution. Thorium was investigated from the actinide series, and it is possible to precipitate about 85% of the thorium as the

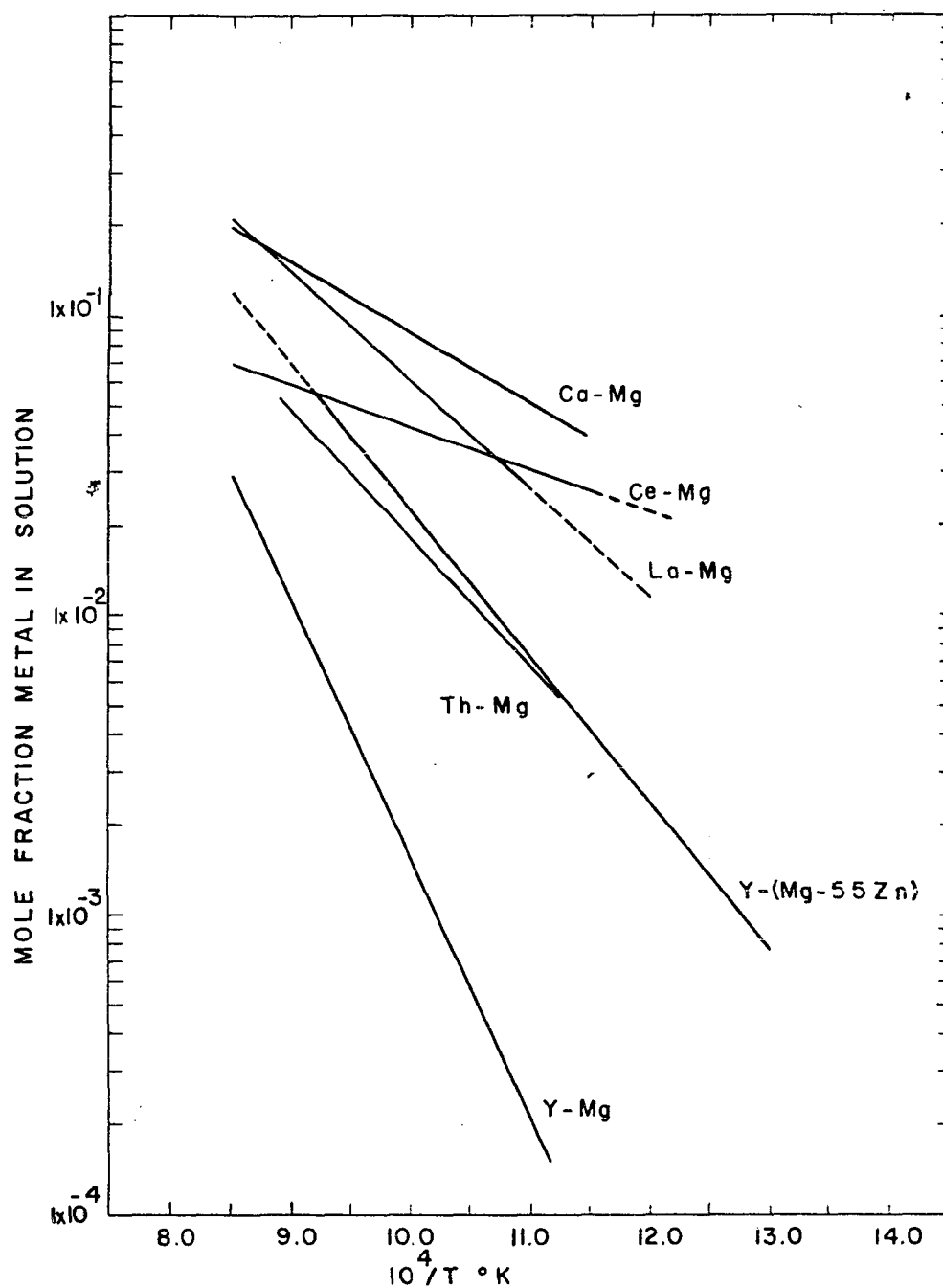


Figure 16. Mole fraction of solute in solution after equilibration with one atmosphere hydrogen as a function of temperature

hydride from Mg - 45 wt. % Th solutions.

The effect of adding other constituents such as zinc and aluminum to the magnesium solutions was also investigated. When zinc was added to form a Mg - 55 wt. % Zn solution, the concentration of yttrium in the solution after equilibration with hydrogen increased from $N_Y = 6.04 \times 10^{-4}$ to $N_Y = 1.19 \times 10^{-3}$ at 675°C. The activity coefficient of yttrium in the Mg-Y solution relative to solid yttrium at 675°C is 0.0311 as compared to 0.00158 for yttrium in the Mg-Zn-Y solution. Although the activity coefficients (given in Table 23) for yttrium relative to solid yttrium for the magnesium-yttrium solutions are less than one, indicating a negative deviation from Raoult's law, a greater negative deviation from Raoult's law is observed as zinc is added. By adding zinc to the solution the interaction between the solute and solvent atoms increases causing an increase in the residual concentration of yttrium in the solution. Further it was found that the yttrium content of a saturated Zn-Y solution was not altered by hydrogen at one atmosphere pressure. Hydrogen had no effect on the solubility of thorium in liquid zinc which was expected from the thermodynamic data for the Th-Zn compounds (50); similarly, hydrogen did not alter the concentration of zirconium in liquid aluminum. Aluminum or zinc when added to the Mg-Th solutions caused the same effect, namely, that the concentration of thorium in the solution increased, indicating a stronger solute-solvent interaction.

Although complete precipitation of these solute metals from the liquid solvents investigated was not realized, reactions of this type might be employed in conjunction with other methods for separating or isolating certain fission impurities in the processing of irradiated fuel materials. For example, it has been shown that uranium-233 produced in thorium as a result of neutron capture can be separated from the thorium simply by dissolving the thorium in liquid magnesium (51). The uranium, is only slightly soluble in the liquid magnesium-thorium solution formed and precipitates as a finely divided solid. After separation of the uranium from the solution it would be possible to precipitate most of the thorium by reacting the Th-Mg solution with hydrogen. Once the thorium is separated as the hydride from the magnesium solution it may be converted to the metal by heating the hydride under reduced pressure. The depleted magnesium solution could be used to extract more thorium.

In general the free energy of formation for the hydrides increases (becomes less negative) as the atomic number increases for metals in a given group. As has been pointed out, other factors being equal, the free energy of formation for the hydride determines to a large extent the degree of precipitation of the solute from the respective solvent. At 700°C the free energies of formation for CaH_2 , SrH_2 , and BaH_2 are -11.4, -4.0 and -0.58 Kcal/mol respectively. Data has

been presented for the precipitation of calcium as the hydride from magnesium solutions at 700°C. Therefore, one would expect the precipitation of Sr or Ba from Mg solutions to be less than that for calcium.

The large difference in the precipitation of yttrium from Mg-Y solutions as compared to the precipitation of La from Mg-La solutions is not particularly surprising, since at 700°C there is about -5.0 Kcal/mol difference between the free energies of formation for these hydrides with yttrium hydride being the more negative.

In the absence of thermodynamic data for scandium hydride and magnesium-scandium compounds, one can only speculate on the effect of hydrogen on Sc-Mg solutions. Since the free energy of formation and the thermal stability of scandium hydride are probably similar to those for yttrium hydride, one would probably expect the behavior of scandium to be similar to yttrium.

Cerium was the metal studied from the rare earth metal series, and about 74% of the metal is precipitated from the magnesium solutions at 700°C. The standard free energy of formation for CeH_2 at 700°C is -12.44 Kcal/mol, which is the least negative value for the rare earth metal hydrides listed below at this temperature. Standard free energies of formation at 700°C for the other rare earth metal hydrides listed in Figure 2 are ErH_2 -17.98, GdH_2 -16.40, SmH_2 -15.50, NdH_2

-15.93, and PrH_2 -15.08 Kcal/mol. In the case of magnesium solutions one would expect (other factors being equal) that erbium and gadolinium would be the more effectively precipitated, followed by neodymium, samarium, and praseodymium. However, sufficient thermodynamic data are not available for these metals to make any accurate predictions on the degree of separation expected.

Although the free energy of formation for ThH_2 at 700°C is only -5.6 Kcal/mol, a considerable amount of the thorium is precipitated from the Th-Mg solutions. This implies that the free energy of formation of the Th-Mg compounds do not represent large negative values. The free energy of formation of PuH_2 at 700°C is about -5.6 Kcal/mol, thus if the interaction between the magnesium and plutonium is of the same order of magnitude as for Th-Mg, one would expect the precipitation of Pu to be of the same order of magnitude.

At one atmosphere pressure UH_3 decomposes at 432°C , which is considerably below the melting point of magnesium. Thus it is not possible to precipitate uranium, which is only slightly soluble in liquid magnesium, from these solutions. No thermodynamic data for the hydrides of the other actinide metals were found.

From the data presented in this investigation, certain qualitative approximations for the precipitation of other metals as the hydride can be made. More thermodynamic data are needed to completely evaluate these systems.

VII. SUMMARY

The precipitation of solute metals as the hydride from various liquid metal solvents has been investigated. The change in solute content as a function of temperature was measured for a number of liquid metal solutions which were equilibrated with hydrogen at one atmosphere pressure. The solvents employed in this investigation were magnesium, aluminum, zinc, Mg - 55 wt. % Zn and Al - 70 wt. % Mg. The effect of hydrogen on the solubility of each of the solutes, calcium, yttrium, lanthanum, cerium, and thorium in liquid magnesium, yttrium and thorium in Mg-Zn, thorium in Al-Mg, and zirconium in aluminum solutions were investigated. The solubility of the various solutes in liquid magnesium for specified temperature ranges is given by the following relations:

$$\log_{10} N_{Ca} = \frac{-2343 \pm 137}{T} + 1.285 \pm 0.137, 625^{\circ} - 900^{\circ}C;$$

$$\log_{10} N_Y = \frac{-8458 \pm 624}{T} + 5.703 \pm 0.605, 650^{\circ} - 913^{\circ}C;$$

$$\log_{10} N_{La} = \frac{-3625 \pm 107}{T} + 2.395 \pm 0.107, 655^{\circ} - 850^{\circ}C;$$

$$\log_{10} N_{Ce} = \frac{-1376 \pm 137}{T} + 0.0028 \pm 0.137, 597^{\circ} - 850^{\circ}C;$$

$$\log_{10} N_{Th} = \frac{-4603 \pm 215}{T} + 2.810 \pm 0.214, 650^{\circ} - 850^{\circ}C.$$

In the above equations N represents the mole fraction of the solute in liquid magnesium.

The solubility of yttrium and thorium in Mg - 55 wt. % Zn solutions and the solubility of thorium in Al - 70 wt. % Mg solutions is given by the following relations:

$$\log_{10} N_Y = \frac{-4857 \pm 134}{T} + 3.199 \pm 0.140, \text{ in Mg - 55 wt. \% Zn,} \\ 485^\circ - 850^\circ\text{C;}$$

$$\log_{10} N_{Th} = \frac{-1880 \pm 30}{T} + 0.558 \pm 0.036, \text{ in Mg - 55 wt. \% Zn,} \\ 500^\circ - 815^\circ\text{C;}$$

$$\log_{10} N_{Th} = \frac{-3441 \pm 91}{T} - 0.152 \pm 0.098, \text{ in Al - 70 wt. \% Mg,} \\ 650^\circ - 850^\circ\text{C.}$$

It has been shown, as the above relations indicate, that the addition of zinc or aluminum to magnesium results in an increase in the residual solute concentration.

The mole fraction of yttrium in the Mg-Zn solvent at 675°C is 1.19×10^{-2} , whereas in the pure magnesium as the solvent at 675°C it is 6.04×10^{-4} . However, the Mg-Zn solvent remains liquid at a lower temperature, thus by lowering the temperature to 484°C the mole fraction of yttrium is 6.04×10^{-4} , which is the same as the concentration of yttrium in the magnesium solution at 675°C . Thus the same degree of separation can be achieved in this case if the reaction temperature is lowered.

Hydrogen had no effect on the solubility of yttrium or

thorium in liquid zinc nor on the solubility of zirconium in liquid aluminum. Hydrogen at one atmosphere pressure also did not precipitate zirconium from liquid U - 5.2 wt. % Cr. solutions containing 2 to 4 wt. % zirconium at 900°C.

Analytical expressions have been derived whereby the activity coefficient (relative to the pure solid solute) of the solute metal in the liquid solvent can be calculated. Negative deviation was observed for all of the solutes with the exception of Th in the Mg-Th and the Mg-Al solutions. These showed a positive deviation from Raoult's law.

It can be concluded from the data obtained in this investigation, that hydrogen at one atmosphere pressure can decrease the solute concentration in specific solvents. Likewise from the scope of this investigation it may be concluded that hydrogen reactions of this nature are limited to the more electropositive metals which form stable hydrides and to solvents of similar electropositive character. Therefore a method such as this cannot be employed as an over-all scheme for processing irradiated fuel material. However, these reactions might be used as a supplement to a reprocessing procedure.

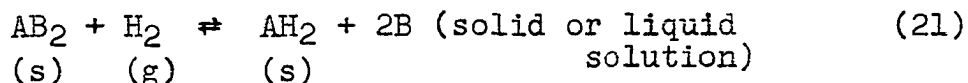
VIII. DETERMINATION OF THERMODYNAMIC PROPERTIES OF INTERMETALLIC COMPOUNDS FROM HYDRIDE REACTIONS

A. Introduction

With the increased effort in the field of pyrometallurgical separations of metals from various liquid-metal solutions, and in the field of metal purification the need for accurate thermochemical data for intermediate phases is important. A number of experimental methods and procedures have been developed for the evaluation of thermodynamic properties for intermediate phases. Kubaschewski and Evans (52), and Chipman and Elliott (53) have described these various methods and the measurements which must be made in order to determine these quantities. The electromotive force method, vapor pressure methods, measurement of distribution coefficients, calorimetric and specific heat methods are among the more commonly used to obtain thermochemical data. The electromotive force method is generally considered to be slightly superior to the other experimental methods, however, in some instances competing side reactions between the fused salt and the container can be very troublesome. Static, dynamic and effusion methods are the common methods employed in vapor pressure studies.

It was the primary purpose of this phase of the research to utilize the information obtained from the hydrides and the

hydrogen reactions from the previous studies to determine if reactions of this nature can be employed to determine the thermodynamic quantities for intermetallic compounds. In this method the equilibrium pressure of hydrogen is measured as a function of temperature for the reaction



This method is limited to systems wherein an equilibrium of this type can be established. Component A reacts with hydrogen gas to form the hydride, whereas B does not react with hydrogen to form the hydride. By equilibrating either the solid compound or a solution containing A or an appropriate mixture of the components with hydrogen gas the above equilibrium may be established. At equilibrium four phases exist and from the phase rule it may be shown that only one degree of freedom remains. Consequently at any given temperature the compositions of the phases and the hydrogen pressure are fixed. The equilibrium constant may be written as

$$K = \frac{[\text{AH}_2][\text{B}]^2}{[\text{AB}_2][\text{H}_2]} = \frac{[\text{B}]^2}{[\text{H}_2]}, \quad (22)$$

since AB_2 and AH_2 are considered to be compounds of fixed composition; the standard free energy change for the reaction may be written as

$$\Delta F^\circ = -RT \ln K = -RT \ln [\text{B}]^2 + RT \ln P_{\text{H}_2} = \Delta F^\circ_{\text{AH}_2} - \Delta F^\circ_{\text{AB}_2}. \quad (23)$$

This expression is equivalent to

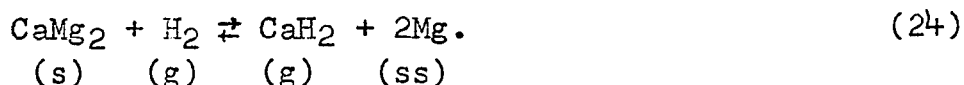
$$-2\overline{\Delta F}_B + RT \ln P_{H_2} = \Delta F^\circ_{AH_2} - \Delta F^\circ_{AB_2}$$

where $\overline{\Delta F}_B$ is the partial molar free energy of solution of B in the liquid or solid solution present at equilibrium. If the standard free energy of formation for the hydride and the partial molar free energy of solution for B are known, then by measuring the equilibrium pressure of hydrogen over the system as a function of temperature, it is possible to calculate the thermodynamic quantities for the compound. If the solution formed is composed primarily of B, one can assume that the activity of B is approximately unity and therefore, $\overline{\Delta F}_B$ can be set equal to zero. This assumption can be applied to systems in which the solubility of A or hydrogen in B is very small.

The calcium-magnesium system was chosen for this investigation. The phase diagram for this system is shown in Figure 6. Features of the system that are desirable from the viewpoint of this investigation are that the composition of the intermediate phase does not vary with temperature and the terminal solid solubility of Ca in Mg is very small. Likewise calcium reacts with hydrogen to form a rather stable crystalline hydride of near stoichiometric composition, whereas magnesium does not form a hydride under these conditions.

Alloys containing about 38 wt. % calcium were used. This composition lies to the left of the composition for the

compound CaMg_2 (see Figure 6), and the equilibrium at temperatures below the eutectic temperature can be expressed as



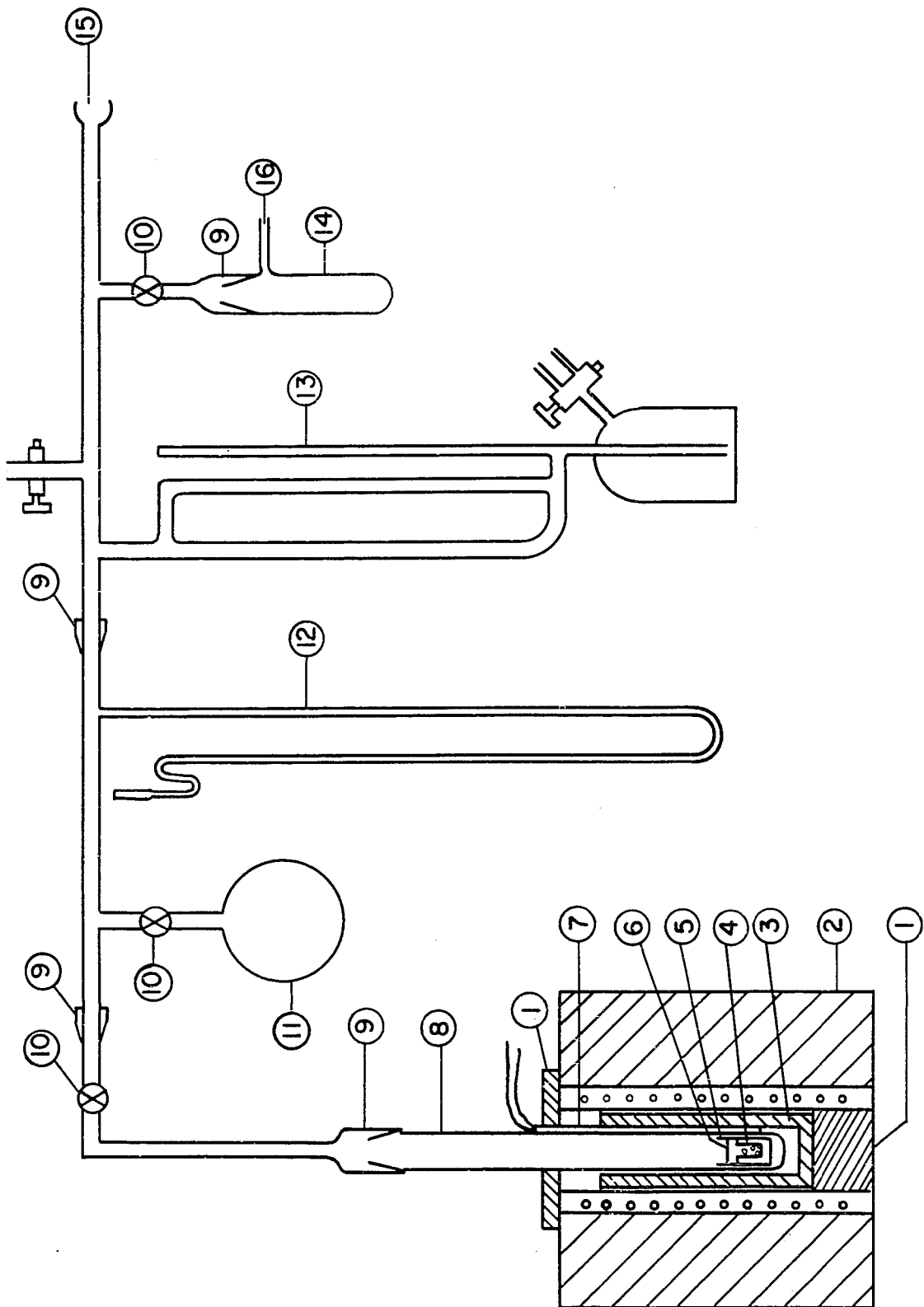
The free energy of formation for CaH_2 is known, therefore, by measuring the pressure of hydrogen over the system as a function of temperature, it is possible to calculate the free energy of formation and the other thermodynamic properties for the compound CaMg_2 . Measurements of the hydrogen pressure were made below the eutectic temperature and above this temperature, namely from 388° to 611°C .

B. Apparatus and Experimental Procedure

A schematic diagram of the system used in this investigation is shown in Figure 17. The entire system was constructed of pyrex glass, except the reaction tube, 8, and the tube used as a container for uranium hydride, 14. These were constructed of quartz. Pressures were measured with either the manometer, 12, or the McLeod gauge, 13. Pressures of the order of 0.03 microns to 40 mm Hg could be measured with the calibrated McLeod gauge. The system was connected to a liquid nitrogen cold-trap, a mercury diffusion pump, and a mechanical pump. Vacuums of the order of 1×10^{-5} mm Hg could be obtained with this system. Prior to an equilibration the system was always checked for leaks. This was done by isolating the system from the vacuum system

Figure 17. Schematic diagram of the system used for measuring the equilibrium hydrogen pressure in the Mg_2Ca equilibrations

1. Fire brick insulation
2. Split-type furnace
3. Stainless steel liner
4. MgO-MgF_2 crucible containing sample
5. Steel crucible - 20 mil walls
6. 1 mil steel foil
7. Alumel-chromel thermocouple
8. Quartz reaction tube
9. Ground glass joint
10. Stopcock
11. 1 liter flask for hydrogen supply
12. Manometer
13. McLeod gauge
14. Quartz tube containing UH_3 for generation of hydrogen gas
15. To vacuum system
16. To hydrogen tank



for several hours, and if no rise in pressure could be noted with the McLeod gauge, it was assumed that there were no leaks in the system.

A split-type resistance furnace was used to heat the reaction tube. To eliminate temperature gradients around the sample, a stainless steel tube, 6 inches long with 1/8 inch walls and a 1/4 inch bottom enclosed a portion of the reaction chamber as shown in Figure 17. A constant temperature zone about 3 inches in length could be maintained with this arrangement. Temperatures were measured with a # 22 B & S alumel-chromel thermocouple, 7, located between the quartz reaction tube and the stainless steel liner. It was held in position by placing it in a slot cut on the inside wall of the stainless steel liner. The temperature was controlled to $\pm 1/2^{\circ}\text{C}$ with a Minneapolis-Honeywell Electronic Recorder and Controller, however, the actual temperature was measured with a Rubicon potentiometer connected to an external galvanometer.

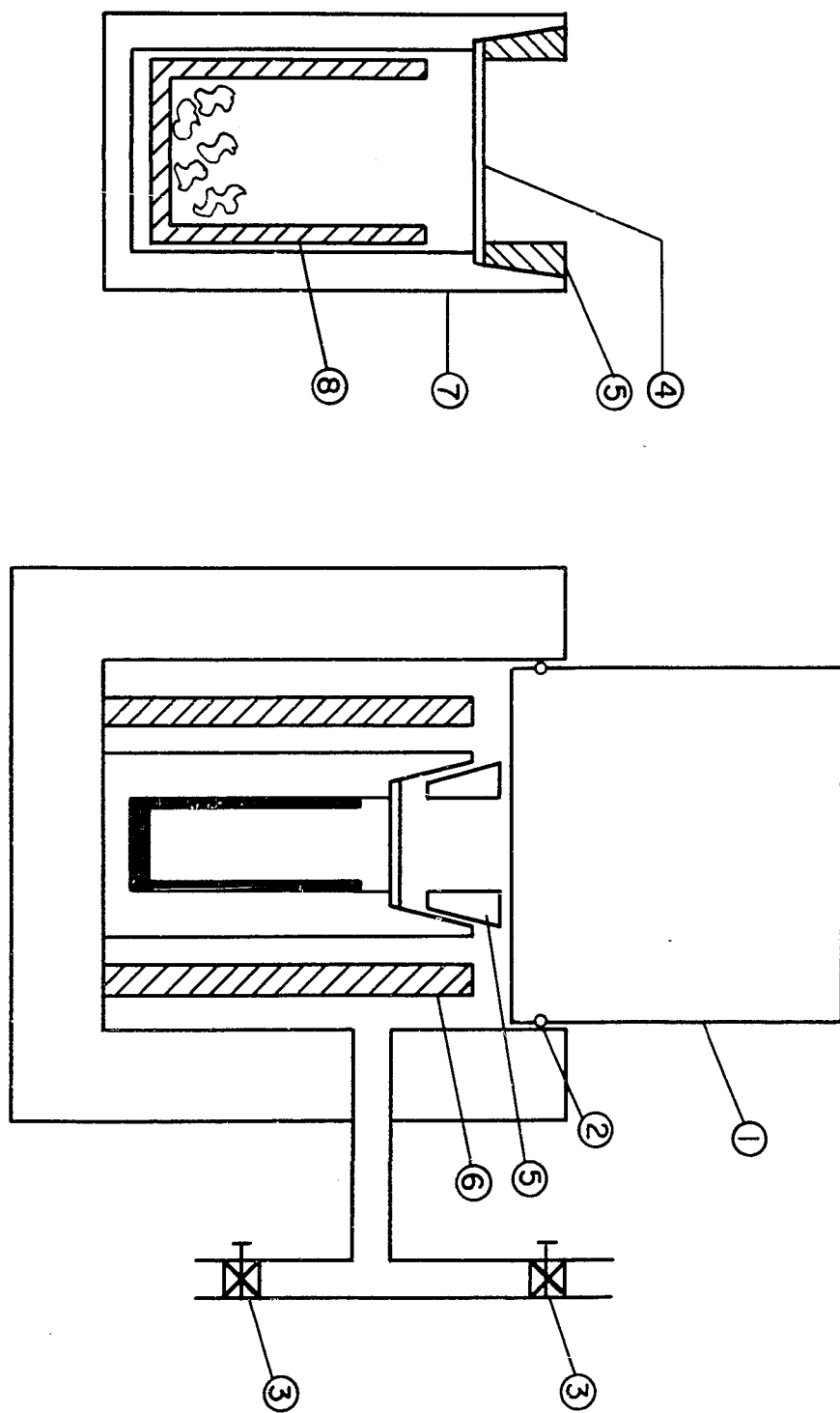
A master alloy of Ca-Mg weighing about 40 grams which contained about 38 wt. % calcium was prepared in a sealed tantalum crucible under a helium atmosphere. To insure adequate mixing and to obtain a homogenous alloy, the metals were heated to 850°C and agitated in a rotating furnace at this temperature for 3 hours. The alloy was then cooled to room temperature. The alloy was crushed in a diamond mortar,

and samples weighing between 2 and 3 grams were used for the equilibrations with hydrogen. The granular sample was contained in a $\text{MgO} - 15 \text{ wt. } \% \text{MgF}_2$ crucible which was $1 \frac{1}{2}$ inches long and $\frac{5}{8}$ inch in diameter. This was placed in $\frac{11}{16}$ inch "O.D." low carbon steel crucible which was 2 inches long with a wall thickness of about 20 mil. A schematic drawing of this assembly is shown in Figure 18. Early in the investigation it was found necessary to restrain the magnesium and calcium vapors over the sample which otherwise sublimed and reacted with the quartz tube. A successful method for capping the steel crucible with 1 mil iron foil, which served as a semi-permeable membrane allowing hydrogen to diffuse in or out but retaining the metal vapors in the crucible, was devised. This was accomplished by cutting a taper on the top inside surface of the steel crucible to a depth of $\frac{3}{8}$ of an inch, leaving a shoulder of about $\frac{1}{16}$ of an inch at the bottom of the taper (see Figure 18). The outer surface of a sleeve cap, 5, was also cut on the same taper to fit in the open end of the crucible. A $\frac{3}{8}$ inch diameter disk cut from one mil iron foil was placed on the $\frac{1}{16}$ inch shoulder, and the cap was fitted in the crucible. The cap was forced down against the iron foil to form a gas tight seal between the cap and the crucible.

A special die, shown in Figure 18, was constructed which permitted one to cap the crucible containing the alloy under

Figure 18. Schematic diagram of crucible and die assembly used to cap the crucible

1. Steel plunger
2. "O" ring to form vacuum seal
3. Pinch clamps
4. One mil iron foil which serves as a partial cap and a semi-permeable membrane
5. Cylindrical cap used to form seal
6. Steel cylinder to stop plunger
7. Low carbon steel crucible, 2 inches long, 3/4 inch "O.D.", with 20 mil walls
8. MgO-MgF_2 porous crucible



a hydrogen atmosphere. The steel crucible, cap, and iron foil were positioned in the steel die and the plunger was inserted. The system was then evacuated by opening the pinch clamp, 3, leading to a vacuum pump. A rubber "O" ring, 2, seated in the plunger formed a vacuum seal between the plunger and die. The die was filled with hydrogen and evacuated several times and then sealed off under one atmosphere of hydrogen pressure by closing both of the pinch clamps. The die was placed in a press and the cap was forced down by the plunger sealing the crucible as described. After the sample had been sealed, it was placed in the quartz tube, 8, Figure 17. The entire system was evacuated and then filled with one atmosphere of purified hydrogen gas. Hydrogen gas used in these equilibrations was obtained from the thermal decomposition of UH_3 . This was done by heating the quartz tube, 14, shown in Figure 17, which contained uranium hydride. The stopcock, 10, to the reserve flask 11, was closed and the system was evacuated again, and isolated from the vacuum system. The desired amount of hydrogen was then admitted to the system by opening the stopcock to the reserve flask. Since the volume of the system had been determined, the volume of hydrogen added was known. Generally enough hydrogen gas was added to react with 50 % of the calcium in the alloy. The system was then heated to the desired temperature and held at this temperature until no

change in the pressure was noted during a period of about 12 hours. This was taken as the equilibrium hydrogen pressure. At temperatures of about 450°C the total time required to reach a constant pressure was about 12 days, at 611°C the time required was about 3 days.

IX. EXPERIMENTAL RESULTS

Measurements of the equilibrium hydrogen pressure above Mg - 38 wt. % Ca alloys were made over a temperature range of 388° to 611°C. The hydrogen pressures measured at various temperatures are tabulated in Table 25. These data are also plotted in Figure 19, in which the logarithm of the pressure expressed in atmospheres is plotted as a function of the reciprocal absolute temperature. The equation for the line drawn in Figure 19 was determined by a least squares treatment and can be expressed as

$$\log_{10} P_{H_2} = \frac{-4667 \pm 139}{T} + 3.357 \pm 0.182. \quad (25)$$

The probable error for the constants are also given in the equation.

An x-ray diffraction pattern was taken with a Debye-Scherrer powder camera of the alloy which was equilibrated with hydrogen to determine if the phases assumed in reaction 4 were actually present. The "d" spacings and the estimated intensities for the observed reflections are listed in Table 26. There appears to be considerable doubt concerning the true lattice for CaH₂. Zintl and Harder (54) report the compound CaH₂ to be orthorhombic having lattice constants of $a_0 = 6.851 \text{ \AA}$, $b_0 = 5.948 \text{ \AA}$, and $c_0 = 3.607 \text{ \AA}$. Hanawalt et al. (55) report the compound to be hexagonal, however, the authors only list the "d" spacings and the relative

Table 25. Equilibrium hydrogen pressure measured over Mg - 38 wt. % Ca alloys

Run number	Hydrogen pressure Atms $\times 10^3$	Temperature	
		$^{\circ}\text{C}$	$10^4/\text{T } ^{\circ}\text{K}$
9	12.509	611	11.30
10	6.707	575	11.82
8	3.047	524	12.55
16	2.443	514	12.71
12	2.606	513	12.72
4	2.200	506	12.84
13	2.100	497	12.99
5	1.692	483	13.23
14	1.150	477	13.33
7	1.381	469	13.47
3	0.918	459	13.66
15	0.752	439	14.04
11	0.178	388	15.13

intensities for the observed reflections. These data are also tabulated in Table 26. Calcium dihydride was prepared by reacting pure calcium metal with excess purified hydrogen gas at elevated temperatures. X-ray data obtained for this material are also listed in Table 26. It was not possible to index the reflections obtained from the prepared calcium

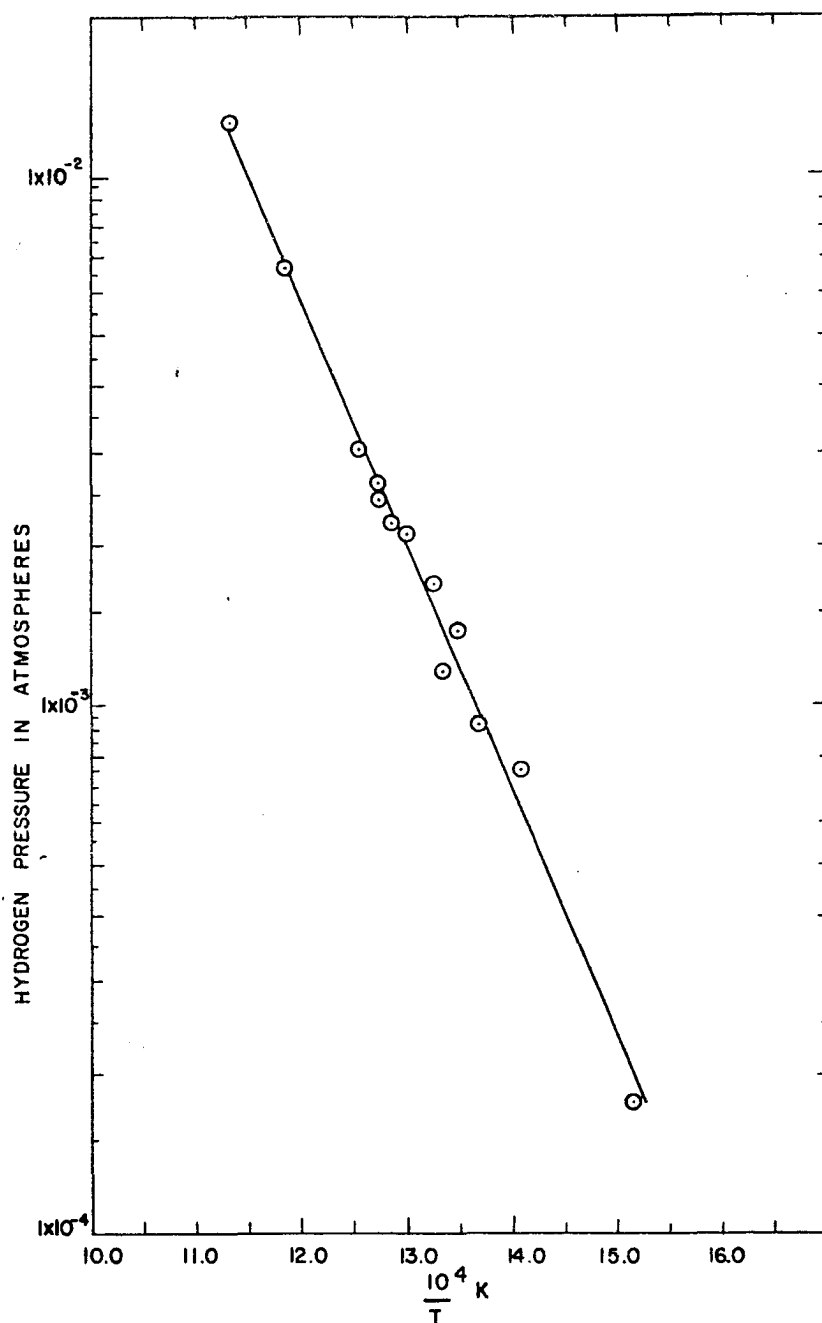


Figure 19. Equilibrium hydrogen pressure measured over Mg - 38 wt. % Ca alloys as a function of temperature

Table 26. X-ray data for CaH_2 , CaMg_2 and Mg - 38 wt. % Ca alloy equilibrated with hydrogen

Alloy		Prepared CaH_2		Literature values CaH_2		Literature values CaMg_2	
Int.	d	Int.	d	Int.	d	Int.	d
S	4.961	M	4.961	8	4.99	44	3.14
W	3.115	W	3.757	40	3.18	75	2.87
S	2.634	S	2.632	100	2.97	100	2.65
VW	1.929	W	2.414	80	2.81	15	2.54
MW	1.800	VW	1.939	8	2.63	8	2.40
VW	1.692	M	1.800	8	2.40	5	2.29
VVW	1.546	W	1.694	40	2.17	5	1.90
VW	1.489	VW	1.564	28	1.92	5	1.80
VW	1.455	VW	1.483	8	1.82	31	1.75
VVW	1.324	VVW	1.319	20	1.79	25	1.70
VVW	1.146	VVW	1.180	24	1.71	20	1.62
VVW	1.064	VVW	1.144	24	1.68	15	1.56
VVW	1.039	VW	1.061	20	1.61	8	1.44
VVW	1.002	VVW	1.036	36	1.54	8	1.37
		VVW	1.014	8	1.48	5	1.34
				4	1.38	3	1.23

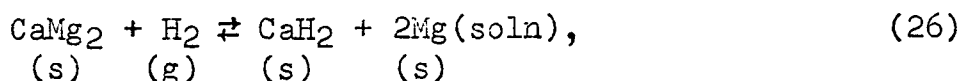
VW	1.692	M	1.800	8	2.40	5	2.29
VVW	1.546	W	1.694	40	2.17	5	1.90
VW	1.489	VW	1.564	28	1.92	5	1.80
VW	1.455	VW	1.483	8	1.82	31	1.75
VVW	1.324	VVW	1.319	20	1.79	25	1.70
VVW	1.146	VVW	1.180	24	1.71	20	1.62
VVW	1.064	VVW	1.144	24	1.68	15	1.56
VVW	1.039	VW	1.061	20	1.61	8	1.44
VVW	1.002	VVW	1.036	36	1.54	8	1.37
		VVW	1.014	8	1.48	5	1.34
				4	1.38	3	1.23
				4	1.35	3	1.21
				36	1.25	3	1.17
				8	1.18	3	1.15
				8	1.15	3	1.13
				4	1.12		
				4	1.07		
				4	1.02		

hydride on the basis of the orthorhombic data given by Zintl and Harder. Fair agreement with Hanawalt's data was observed. The "d" spacings for the reflections from the alloy can be satisfactorily accounted for on the basis of the "d" spacings for the compound CaMg_2 (also listed in Table 26), and those observed for the prepared CaH_2 . The second reflection listed for the prepared hydride, which does not agree with the data listed for the alloy or CaH_2 , compares quite well with a reflection for quartz. This reflection could have been obtained from the quartz fiber used to hold the sample. It can be concluded that the calcium hydride which was prepared is the same material as that obtained in the alloy after equilibration with hydrogen, and the alloy contains CaH_2 in addition to magnesium and the compound CaMg_2 . No reflections for the magnesium-rich solid solution were observed in the x-ray pattern, this is probably due to the fact that as the calcium reacts with the hydrogen, the magnesium which remains sublimes from the alloy and condenses on the under side of the iron foil. The condensed material on the foil was examined microscopically, and appeared to be crystallites of pure magnesium with a small amount of the Mg-Ca eutectic. Although the bulk of the magnesium-rich phase was not in direct contact with the remainder of the alloy which x-ray patterns showed was

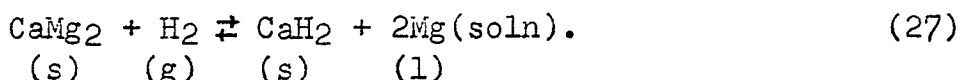
predominately CaH_2 and CaMg_2 , equilibria between the solid phases could still be attained through the vapor phase.

X. THERMODYNAMIC CALCULATIONS AND DISCUSSION

The equilibrium reaction which was investigated at temperatures below the eutectic horizontal can be expressed as



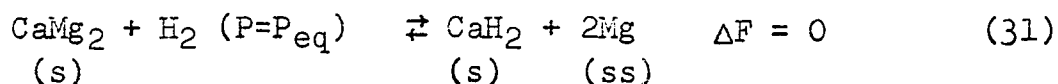
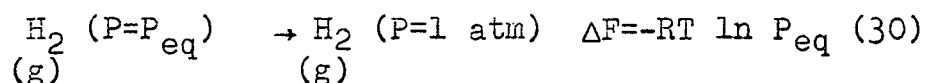
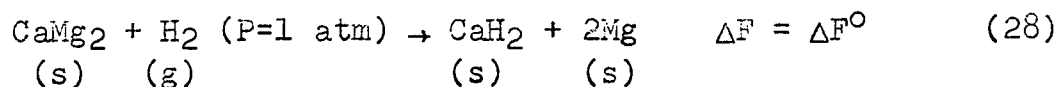
and for temperatures above the eutectic horizontal the following reaction will apply



For reaction 26 magnesium-rich solid solution is formed, whereas in reaction 27 magnesium-rich liquid solution is formed. There are three components (Mg, Ca, and H₂) and four phases (CaMg₂, H₂, CaH₂, and Mg solid solution below the eutectic temperature or Mg liquid solution above the eutectic horizontal). Therefore from the phase rule, $F = 3 - 4 + 2$, the system is univariant or there is one degree of freedom, indicating that it is possible to arbitrarily fix, within limits, either the temperature or the pressure, after which all the other intensive properties of each phase of the system become determinate. For the reaction investigated the temperature was fixed, therefore, at equilibrium the pressure should remain constant at a fixed value as indicated by the phase rule. By measuring the equilibrium hydrogen pressure over the system as a function of temperature, it is possible to calculate all of the thermodynamic quantities

for the compound CaMg_2 .

Reaction 26, the equilibrium investigated below the eutectic temperature can be obtained by combining the following equations.



At equilibrium one can write

$$\Delta F^\circ + 2\overline{\Delta F}_{\text{Mg}} - RT \ln P_{\text{eq}} = 0 \quad (32)$$

where ΔF° is the standard free energy change for reaction 28, which can be expressed as $\Delta F^\circ = \Delta F^\circ_{\text{CaH}_2} - \Delta F^\circ_{\text{CaMg}_2}$. The solid solubility of Ca in Mg is very small as indicated by the Mg-Ca phase diagram (see Figure 6). Therefore one can assume that the magnesium solid solution is essentially pure magnesium in its standard state and the activity of magnesium can be set equal to one. Thus $\overline{\Delta F}_{\text{Mg}}$, the partial molar free energy of solution, is equal to zero. Equation 32 can now be expressed as

$$\Delta F^\circ_{\text{CaMg}_2} = \Delta F^\circ_{\text{CaH}_2} - RT \cdot 2.3 \log_{10} P_{\text{eq}} \quad (33)$$

The standard free energy of formation for CaH_2 can be expressed as $\Delta F^\circ = 4.575 T \log_{10} P_{\text{H}_2}$. The dissociation pressure reported by Johnson et al. (22) for the system consisting of equal amounts of CaH_2 and solid solution of hydrogen in calcium can be expressed by the relation

$$\log_{10} P_{\text{H}_2} \text{ atm} = \frac{-10870}{T} + 8.612 \quad (34)$$

Substituting equation 34 for $\log_{10} P_{\text{H}_2}$ in the above equation gives the following equation

$$\Delta F^\circ_{\text{CaH}_2} = -49,730 + 39.40 T \quad (35)$$

for the standard free energy of formation for CaH_2 . Substituting equation 35 for $\Delta F^\circ_{\text{CaH}_2}$ and equation 25, the expression for the measured hydrogen pressure over the system, for $\log_{10} P_{\text{eq}}$ in equation 33 gives the following expression

$$\Delta F^\circ_{\text{CaMg}_2} = -28,378 + 24.042 T, \quad (36)$$

which can be used to calculate the standard free energy of formation for the compound Mg_2Ca . From thermodynamics it can be shown that $\frac{d(\Delta F^\circ/T)}{d(1/T)} = \Delta H^\circ$ (56). Thus dividing equation 36 by T and differentiating the equation with respect to $1/T$, gives -28.378 Kcal/mol for the standard enthalpy of formation for CaMg_2 . The entropy of formation can be obtained from the relation $\Delta F^\circ = \Delta H^\circ - T\Delta S^\circ$, which was found to be -24.042 eu/mol . The thermodynamic properties for CaMg_2 have been calculated at several temperatures from equation 36, and are tabulated in Table 27, along with values obtained by

other investigators for comparison. Values for the enthalpy of formation of CaMg_2 have been tabulated as -30 Kcal/mol by Rossini et al. (57) and -21.3 Kcal/mol by Kubaschewski and Evans (52). These values are based on the data obtained by Biltz and Hohorst (58) from solution calorimetry. Rossini and Kubaschewski did not report values for ΔF° or ΔS° . Smith and Smythe (59) have determined the enthalpy of formation for CaMg_2 by measuring the vapor pressure of magnesium over alloys by the Knudsen effusion method. They report a value of -8.3 ± 2.9 Kcal/mol. The enthalpy of formation, ΔH° , for CaMg_2 obtained in this investigation is considerably higher than Smith and Smythe's value but agrees very well with the -30 Kcal/mol tabulated by Rossini et al. At 600°C the ΔF° shows good agreement, however, at lower temperatures a larger difference is observed. The reason for the large differences between the ΔH° and ΔS° obtained by Smith and Smythe with the Knudsen effusion method and the values obtained in this research is not known. However, the temperature range for their measurements was only 655° to 718°K , or 63 degrees, whereas in the present investigation the temperature range was 661° to 790°K , or 129 degrees. The determination of the enthalpy is very sensitive to errors in the slope of the curves drawn through the data points. It would be advantageous to check these data by an independent method such as the heats of combustion using a bomb

Table 27. Thermodynamic properties of CaMg_2

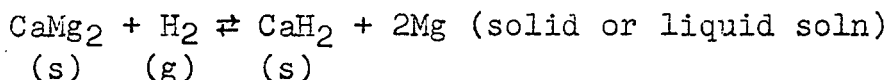
Temperature $^{\circ}\text{C}$ $^{\circ}\text{K}$		$-\Delta F^{\circ}$ Kcal/mol	$-\Delta H^{\circ}$ Kcal/mol	$-\Delta S^{\circ}$ cal/mol- $^{\circ}\text{K}$	Reference
25	298	21.22	28.4	24.02	This investigation
400	673	12.19	28.4	24.02	
500	773	9.81	28.4	24.02	
600	873	7.39	28.4	24.02	
25	298	7.97	8.3	1.1	Smith and Smythe (59)
400	673	7.56	8.3	1.1	
500	773	7.45	8.3	1.1	
600	873	7.34	8.3	1.1	
25	298		30.0		Rossini <u>et al.</u> (57)
25	298		21.3		Kubaschewski and Evans (52)

calorimeter.

As was previously pointed out, this hydride method has certain limitations, but could very probably be used to determine the thermodynamic properties for the rare earth metal-magnesium compounds. These systems appear to be attractive since the rare earth metals form rather stable hydrides, and the data presented on the hydrides appears to be reliable.

XI. SUMMARY

A method has been presented wherein the thermodynamic properties for intermediate phases can be obtained from hydride reactions. This method was used to determine the thermodynamic properties for the compound CaMg_2 . The equilibrium hydrogen pressure was measured over a temperature range of 388° to 611°C for the following reaction.



It has been shown by x-ray diffraction techniques and by microscopic examination of the equilibrated alloy, that the phases specified by the reaction were present. Thus it is possible to calculate all of the thermodynamic quantities for the compound simply by measuring the equilibrium hydrogen pressure over the system as a function of temperature. The free energy of formation of the compound in cal/mol can be expressed as

$$\Delta F^\circ = -28,378 + 24.042 T.$$

The enthalpy and entropy of formation at 298°K for CaMg_2 obtained in this investigation were -28.378 Kcal/mol and -24.042 eu/mol respectively. The value obtained for the enthalpy of formation of CaMg_2 agrees very well with the value tabulated by Rossini et al. (57), however, this value is considerably higher than the value reported by Smith and Smythe (59) from Knudsen effusion experiments. No explanation can

be given at the present for the large difference between these values, however, since the value reported in this investigation agrees with the value obtained from another investigation determined by an entirely different method, it is felt that these values represent a reliable figure for the enthalpy of formation for CaMg_2 . In order to resolve this difference an independent check on the enthalpy of formation of CaMg_2 could be made by bomb calorimetry using heats of combustion.

XII. LITERATURE CITED

1. Martin, F. S., and Miles, G. L., Chemical Processing of Nuclear Fuels, New York, Academic Press, Inc. (1958).
2. Chiotti, P., and Voigt, A. F., Proceedings of the Second United Nations International Conference on the Peaceful Uses of Atomic Energy, 17: 368 (1958).
3. Dennis, W. H., Metallurgy of Non-Ferrous Metals, 1st ed. London, Sir Isaac Pitman and Son, Limited. (1954).
4. Paneth, F., Radio Elements as Indicators and Other Selected Topics in Inorganic Chemistry, New York, McGraw-Hill Book Company. (1928).
5. Gibb, T. R. P., Jr., Journal of Chemical Education, 25: 577 (1948).
6. Hurd, D. T., Chemistry of the Hydrides, New York, John Wiley and Sons, Inc. (1952).
7. Dialer, D., Monatsh., 79: 311 (1948).
8. Libowitz, G. G., and Gibb, T. R. P., Jr., The Journal of Physical Chemistry, 60: 510 (1956).
9. Morrison, C. R., Pressau, J. P., Joyner, P. A., and Adams, R. M., Synthesis of Magnesium Hydride. U. S. Atomic Energy Commission Report CCC-1024-Tr-19 [Callery Chemical Company, Penna.] (April 1954).
10. Holley, C. E., Jr., and Lemons, J. F., The Preparation of the Hydrides of Magnesium and Beryllium. U. S. Atomic Energy Commission Report LA-1600 [Los Alamos Scientific Lab., N. Mex.] (April 1954).
11. Finhalt, A. E., Bond, A. C., Jr., and Schlesinger, H. I., Journal American Chemical Society, 69: 1199 (1947).
12. Barbaras, G. D., Dillard, C., Finhalt, A. E., Wartck, T., Wilzbach, K. E., and Schlesinger, H. I., Journal of American Chemical Society, 73: 4585 (1951).
13. Messer, C. E., Homonoff, H., Nicherson, R. F., and Gibb, T. R. P., Jr., Light Metal Hydrides for Shielding. U. S. Atomic Energy Commission Report NYO-3955 [New York Operations Office, AEC] (1953).

14. Banus, M. D., and Bragden, R. W., A Survey of Hydrides for Use in the ANP Program. U. S. Atomic Energy Commission Report CF-52-2-212 [Oak Ridge National Lab. Tenn.] (February 1, 1952).
15. Elson, R. E., Hornig, H. C., Jolly, W. L., Kurry, J. W., Ramsey, W. J., and Zalkin, A., Some Physical Properties of the Hydrides. U. S. Atomic Energy Commission Report UCRL-4519 [California. Univ., Livermore. Radiation Lab.] (1955).
16. Bost, W. E. Metal Hydrides. U. S. Atomic Energy Commission Report TID-3610 [Technical Information Service, AEC] (1958).
17. Metals Hydride Incorporate, A Bibliography on the Hydrides of Metals and Metalloids. U. S. Atomic Energy Commission Report NP-4716 [Technical Information Service, AEC] 3rd Supplement (1952).
18. Herold, A., Compt. Rend. 228: 249 (1947).
19. Herold, A., Compt. Rend. 228: 687 (1949).
20. Coates, G. E., and Glockling, F., Journal Chemical Society, London, 2526 (1954).
21. Treadwell, W. D., and Stecher, J., Journal Helvetica Chemica Acta, 36: 1820 (1953).
22. Johnson, W. C., Stubbs, M. F., Sidwell, A. E., and Peahukas, A., Journal American Chemical Society, 61: 318 (1939).
23. Guntz, A., Compt. Rend. 134: 838 (1902).
24. Gibb, T. R. P., Jr., Hydrides and Metal-Hydrogen Systems. U. S. Atomic Energy Commission Report NEPA-1841 [Fairchild Engine and Airplane Corp. NEPA Div. Oak Ridge Tenn.] (April 30, 1951).
25. Los Alamos Scientific Laboratory and University of California Radiation Laboratory, Excerpts from Los Alamos Scientific Laboratory and University of California Radiation Laboratory. U. S. Atomic Energy Commission Report WASH-729 [Atomic Energy Commission, Washington, D. C.] (1956).
26. Mulford, R. N. R., and Holley, C. E., Jr., Journal Physical Chemistry, 59: 1222 (1955).

27. Sturdy, G. E., and Mulford, R. N. R., *Journal American Chemical Society*, 78: 1083 (1956).
28. Mulford, R. N. R., A Review of the Rare Earth Hydrides. *United States Atomic Energy Commission Report AECU-3813* [Technical Information Service, AEC] (1958).
29. Nottorf, R. W., *Journal of Science*, 26: 26 (1952).
30. Mallet, M. W., and Campbell, I. E., *Journal American Chemical Society*, 73: 4850 (1951).
31. Mulford, R. N. R., and Sturdy, G., *Journal American Chemical Society*, 77: 3449 (1955).
32. Gibb, T. R. P., Jr., *Journal American Chemical Society*, 73: 1750 (1951).
33. Gulbransen, E. A., and Andrew, K. F., *Journal of the Electro-chemical Society*, 101: 474 (1954).
34. Gilbert, P. T., Jr., General Chemistry Quarterly Progress Report, U. S. Atomic Energy Commission Report NAA-SR-1205 [North American Aviation, Inc., Downey, California] (July - Sept., 1954).
35. Albrecht, W. M., and Goode, W. D. Studies of Uranium and Uranium-Alloy Fuels. U. S. Atomic Energy Commission Report BMI-1267 [Battelle Memorial Inst. Columbus, Ohio] (1958).
36. Kelley, K. K., U. S. Bureau of Mines Bulletin 383, (1935).
37. Yost, D. M., and Russel, H., Systematic Inorganic Chemistry, New York, Prentice-Hall, (1946).
38. Sherman, R. H., and Gianqul, W. F., *Journal American Chemistry Society*, 77: 2154 (1955).
39. Hansen, M., Constitution of Binary Alloys, New York, McGraw-Hill Book Company, Inc. (1958).
40. Gibson, E. D., and Carlson, O. N., *American Society for Metals Transactions*, Preprint Vol. 52, No. 146, (1959).
41. Willard, H. H., and Gordon L. *Analytical Chemistry*, 20: 165 (1948).

42. Fritz, J. S., Oliver, R. T., and Pietrzyk, D. J., Analytical Chemistry, 30: 1111 (1958).
43. Banks, C. V., and O'Laughlin, J. W., Analytical Chemistry, 28: 1338 (1956).
44. Diehl, H., and Ellingboe, J. L., Analytical Chemistry, 28: 882 (1956).
45. Fritz, J. S., and Johnson, M., Analytical Chemistry, 27: 1653 (1955).
46. DeFayette, R. W., Kinetics of the reaction between yttrium and water vapor, unpublished M. S. thesis, Ames, Iowa. Library, Iowa State University of Science and Technology. (1959).
47. Gill, K. J., Research Associate, Atomic Energy Commission, Ames Laboratory, Ames, Iowa. Information on the Yttrium-Zinc Phase Diagram. Private communication. (1959).
48. Kubaschewski, O., and Catterall, J. A., Thermochemical Data of Alloys, London, Pergamon Press. (1956).
49. Woerner, P. F., and Chiotti, P., Precipitation of Thorium Hydride from Thorium-Magnesium Solutions. U. S. Atomic Energy Commission Report ISC-928 [Ames Lab., Ames, Iowa] (1957).
50. Gill, K. J., Research Associate, Atomic Energy Commission, Ames Laboratory, Ames, Iowa. Information on the Th-Zn Compounds. Private communication. (1959).
51. Chiotti, P., and Shoemaker, H. E., Industrial and Engineering Chemistry, 50: 137 (1958).
52. Kubaschewski, O., and Evans, E. L., Metallurgical Thermochemistry, New York, Pergamon Press. (1958).
53. Chipman, J., and Elliott, J. F., Thermodynamics in Physical Metallurgy, Cleveland, Ohio, American Society for Metals (1952).
54. Zintl, E., and Harder, A., Zeitschrift fur Electrochemie, 41: 33 (1935).
55. Hanawalt, J. D., Rinn, H. W., and Frevel, L. K., Analytical Chemistry, 10: 457 (1938).

56. Darken, L. S., and Gurry, R. W., Physical Chemistry of Metals, New York, McGraw-Hill. (1953).
57. Rossini, F., Wagman, D. D., Evans, W. H., Levine, S., and Jaffe, I., Selected Values of Chemical Thermodynamic Properties, National Bureau Standards Circular 500 (1952).
58. Biltz, W., and Hohorst, G., Zeitschrift fur Anorganische und Allgemeine Chemie, 121: 1 (1922).
59. Smith, J. F., and Smythe, R. L., Acta Metallurgica, 7: 261 (1959).

XIII. ACKNOWLEDGMENTS

The author wishes to express his sincere appreciation to Dr. Premo Chiotti for his helpful counsel and advice during the course of this investigation and in the preparation of this manuscript.

The author wishes to thank Ralph Curtis for his contributions to the experimental work contained in this report and Forest Ellson for his help in constructing the apparatus.

Finally the author wishes to express his appreciation to the entire metallurgy group for their helpful discussion of this problem.